5-2013

Turnover Rate Of The Neuronal Connexin Cx36 In Hela Cells

Yanran Wang

Turnover rate of the Neuronal Connexin Cx36 in HeLa Cells

by

Yanran Wang

APPROVED:

_____

Supervisory Professor: John O'Brien, PhD

_____

Joseph L. Alcorn, PhD

_____

Steve Massey, PhD

_____

Christophe P. Ribelayga, PhD

_____

Eric C. Swindell, PhD

APPROVED:

_____

Dean, The University of Texas
Graduate School of Biomedical Sciences at Houston

TURNOVER RATE OF THE NEURONAL CONNEXIN CX36 IN HELA CELLS

A THESIS

Presented to the Faculty of
The University of Texas
Health Science Center at Houston
and
The University of Texas
MD Anderson Cancer Center
Graduate School of Biomedical Sciences
in Partial Fulfillment

of the Requirements

for the Degree of

MASTER OF SCIENCE

by

Yanran Wang
Houston, Texas

May, 2013

Turnover rate of the neuronal connexin Cx36 in HeLa cells

Publication No. _____

Yanran Wang

Supervisory Professor: John O'Brien, PhD

Electrical synapses formed of the gap junction protein Cx36 show a great deal of functional plasticity, much dependent on changes in phosphorylation state of the connexin. However, gap junction turnover may also be important for regulating cell-cell communication, and turnover rates of Cx36 have not been studied. Connexins have relatively fast turnover rates, with short half-lives measured to be 1.5 to 3.5 hours in pulse-chase analyses of connexins (Cx26 and Cx43) in tissue culture cells and whole organs. We utilized HaloTag technology to study the turnover rate of Cx36 in transiently transfected HeLa cells. The HaloTag protein forms irreversible covalent bonds with chloroalkane ligands, allowing pulse-chase experiments to be performed very specifically. The HaloTag open reading frame was inserted into an internal site in the C-terminus of Cx36 designed not to disrupt the regulatory phosphorylation sites and not to block the C-terminal PDZ interaction motif. Functional properties of Cx36-Halo were assessed by Neurobiotin tracer coupling, live cell imaging, and immunostaining. For the pulse-chase study, transiently transfected HeLa cells were pulse labeled with Oregon Green (OG) HaloTag ligand and chase labeled at various times with tetramethylrhodamine (TMR) HaloTag ligand. Cx36-Halo formed large junctional plaques at sites of contact between transfected HeLa cells and was also contained in a large number of intracellular vesicles. The Cx36-Halo transfected HeLa cells supported Neurobiotin tracer coupling that was regulated by activation and inhibition of PKA in the same manner as wild-

type Cx36 transfected cells. In the pulse-chase study, junctional protein labeled with the pulse ligand (OG) was gradually replaced by newly synthesized Cx36 labeled with the chase ligand (TMR). The half-life for turnover of protein in junctional plaques was 2.8 hours. Treatment of the pulse-labeled cells with Brefeldin A (BFA) prevented the addition of new connexins to junctional plaques, suggesting that the assembly of Cx36 into gap junctions involves the traditional ER-Golgi-TGN-plasma membrane pathway. In conclusion, Cx36-Halo is functional and has a turnover rate in HeLa cells similar to that of other connexins that have been studied. This turnover rate is likely too slow to contribute substantially to short-term changes in coupling of neurons driven by transmitters such as dopamine, which take minutes to achieve. However, turnover may contribute to longer-term changes in coupling.

Table of Contents

LIST OF FIGURES/TABLES

LIST OF ABBREVIATIONS

BFA: Brefeldin A

CE: Club Ending

CT: C-terminal

Ctrl: Control

Cx: Connexin

DMSO: Dimethyl Sulfoxide

ER: Endoplasmic Reticulum

EPSP: Excitatory Postsynaptic Potential

Halo-EV: HaloTag Empty Vector

IPL: Inner Plexiform Layer

MEM: Minimum Essential Medium

OG: Oregon Green

OPL: Outer Plexiform Layer

PBS: Phosphate Buffered Saline

PBST: Phosphate Buffered Saline with Tween 20

PKA: Protein Kinase A

PM: Plasma Membrane

ROI: Region of Interest

Rp: Rp-8-cpt-cAMPS

Sp: Sp-8-cpt-cAMPS

TGN: trans-Golgi network

TMR: Tetramethylrhodamine

Introduction

In the nervous system, neurons pass information through synapses. There are two main modalities of synaptic transmission: through chemical synapses and through electrical synapses. In chemical synapses, there are distinct pre-synaptic and post-synaptic sides. The pre-synaptic side releases chemical transmitters, known as neurotransmitters, which diffuse across the cleft. The neurotransmitters bind to and then activate specific post-synaptic receptors, which in turn generate downstream responses. Electrical synapses, on the other hand, consist of gap junctions that provide a direct pathway of low resistance. Regulation and trafficking of ion channels and receptor proteins in chemical synapses have been well studied and have been proven to be an important aspect of synaptic strength and plasticity. However, little is known about what contributes to modulating electrical synaptic plasticity. It has been shown that electrical synapses are dynamic and possess plastic properties and turnover of gap junction proteins could play an important role. In this study, we focused on the turnover rate of Cx36, an important gap junction protein in electrical synapses. Understanding the trafficking and regulation of Cx36 will be an important first step in understanding whether connexin turnover rate affects electrical synaptic plasticity.

1. **Connexin 36 Gap Junctions**

Gap Junctions are composed of membrane proteins that form a specialized intercellular channel that connects the cytoplasm of two adjacent cells. They allow direct transfer of ions and small molecules including metabolites and second messengers (Saez et al., 2003). Connexins were identified as the proteins comprising gap junctions in vertebrates, and they are diverse and ubiquitous. There are 21 connexin genes in the human

genome and 20 in the mouse genome (Willecke et al., 2002). Connexins have four trans-membrane domains, two extracellular loops and one intracellular loop. Both the carboxyl terminus (C-terminus) and amino terminus (N-terminus) are in the cytoplasm. Six connexins oligomerize to form a hexameric structure called a connexon, or a hemichannel. Each hemichannel can contain only one type of connexin subunit (homomeric) or a mixture of different connexin subunits (heteromeric). Two connexons from adjacent cells dock together to form a functional gap junction channel; the process is known as gap junction coupling. The association of two connexons into gap junctions can be between the same two connexon (homotypic) or of connexons with different subunit compositions (heterotypic) (Figure 1) (Bloomfield and Volgyi, 2009).

A.
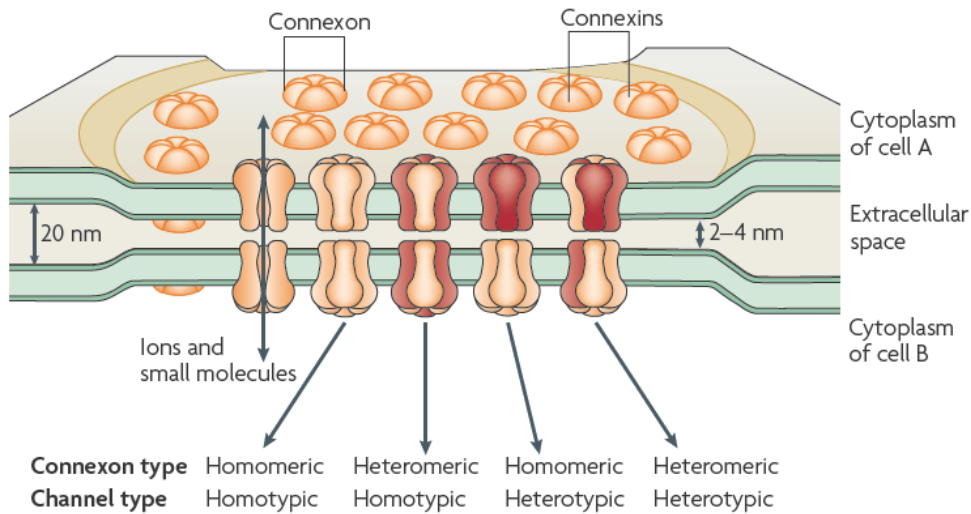
B.
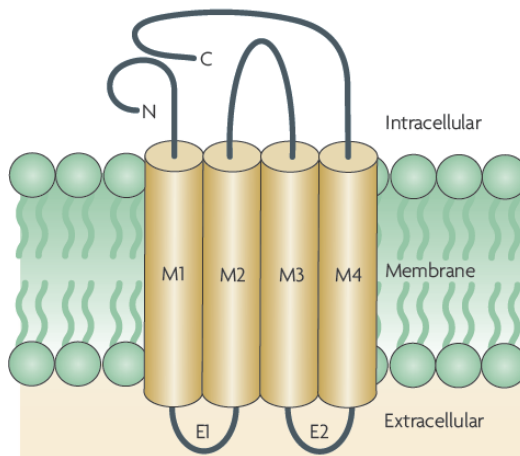
Figure 1: structure and molecular organization of gap junctions. A) Formation of gap junction between two cells and various gap junction types. B) Ribbon structure of a typical connexin. From Bloomfield and Volgyi, 2009 (Originally published in Nature Review Neuroscience).

Although the connexin gene family is large, Cx36 (Cx35 is the non-mammalian homolog) is the predominant connexin that forms electrical synapses in neurons. It is widespread in the central nervous system (Condorelli et al., 2000), including retina (Deans et al., 2002), olfactory bulb (Christie et al., 2005), neocortex (Deans et al., 2001) (Blatow et

al., 2003), hippocampus (Belluardo et al., 2000; Hormuzdi et al., 2001) (Belluardo et al., 2000), inferior olive (Long et al., 2002) (De Zeeuw et al., 2003), and cerebellum (Belluardo et al., 2000). Cx36 has very low voltage sensitivity (Srinivas et al., 1999) (Al-Ubaidi et al., 2000). It is very cation selective, and it has nearly the smallest single channel conductance of any connexin (~15pS) (Srinivas et al., 1999).

Cx36 gap junction coupling is regulated by protein kinase A activity. In early scrape loading experiments using HeLa cells stably transfected with wild-type Cx36, treatment of PKA activator Sp-8-cpt-cAMPS (Sp) decreased Cx36 coupling, while treatment of PKA inhibitor Rp-8-cpt-cAMPS (Rp) increased coupling (Ouyang et al., 2005) (Figure 2A-D). Scrape loading experiments using transiently transfected HeLa cells (unpublished data from O'Brien lab) show similar result in Rp treated condition, but failed to reduce coupling while treated with Sp, possibly due to activation of phosphatases by the transfection reagent (Figure 2E). In the transiently transfected HeLa cells, the control and Sp conditions gave a background coupling that was comparable to non-transfected HeLa cells. This background coupling of HeLa cells can be explained by a recent publication by Marandykina et al. In the Marandykina study, it showed that Cx36 gap junction coupling in HeLa transfectants can be inhibited by the presence of endogenous arachidonic acid, which stabilizes a closed conformation state of the channel that leads to low fraction of functional channels. Transfection reagent could be activating a phospholipase pathway, or lipids in the transfection reagent could be causing uncoupling directly (Marandykina et al., 2013). In tracer coupling experiments done in both non-transfected and empty vector transfected cells, there is still coupling observed when treated with PKA activator, probably due to the background coupling by other connexins.
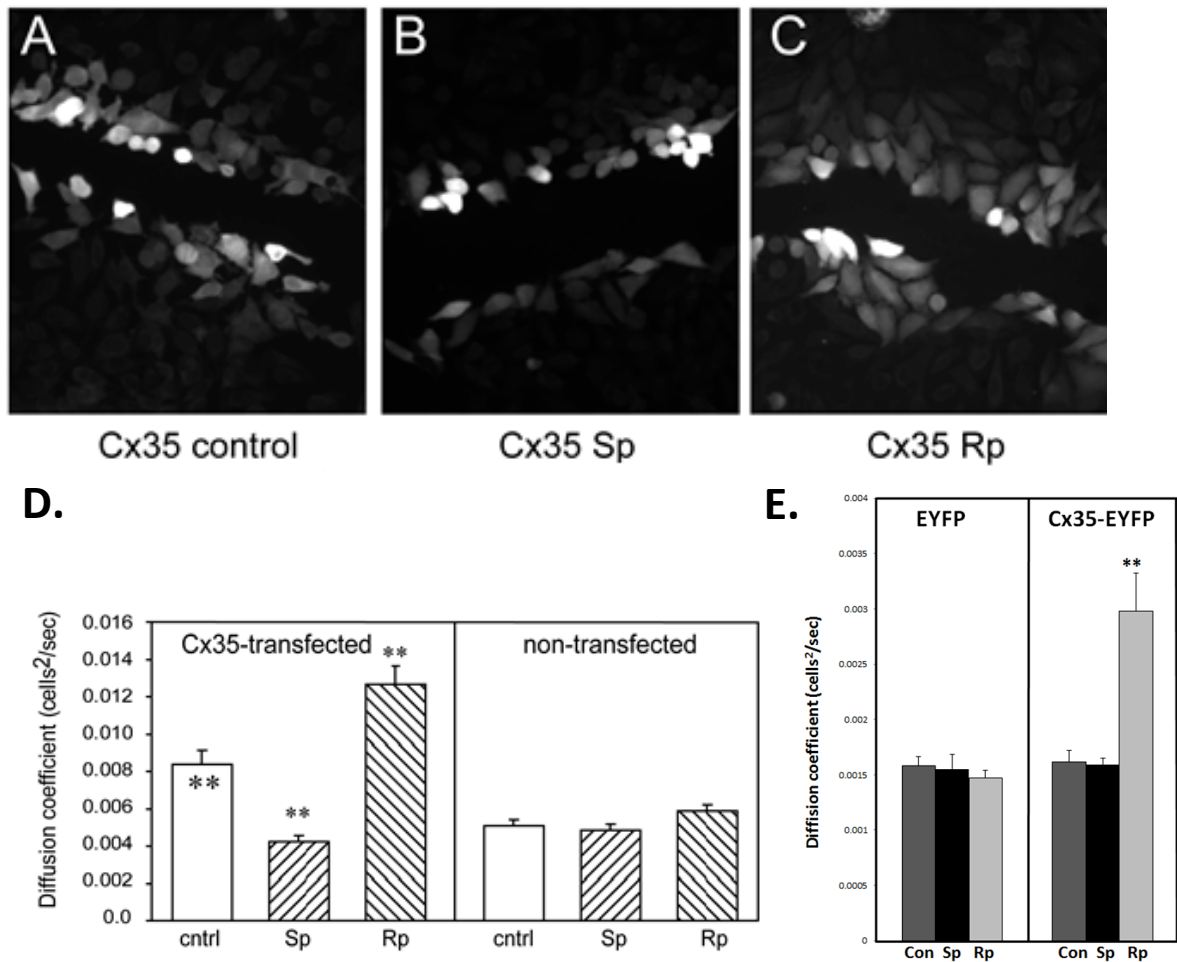
Figure 2: Effects of PKA activation and inhibition on tracer coupling in Cx35-HeLa cells measured by scrape-loading. (A-D) from Ouyang et al., 2005 (Originally published in Brain Research. Molecular Brain Research. (E) unpublished data from O'Brien Lab.

Cx36 is regulated by PKA at two major regulatory sites, Ser110 in the intracellular loop and Ser293 (S276 in Cx35) in the C-terminus (Figure 3A). Phosphorylation of these two sites is critical in regulation of coupling mentioned in the figure above (Ouyang et al., 2005) (Kothmann et al., 2007). The Intracellular loop also harbors Cam Kinase binding site (Alev et al., 2008). Ser315, located towards the end of the C-terminus, has long been an important candidate in possibly assembling a protein complex that contributes to the phosphorylation states of the regulatory sites (Figure 3B). Ser315 is phosphorylated by

CamKII (Alev et al., 2008), and Ouyang et al. showed that mutation at Ser315 (S298 in Perch Cx35) invert the coupling mechanism when measured by tracer coupling in HeLa cells (Ouyang et al., 2005). However preserving Ser315 alone was not enough to prevent inversion of the coupling mechanism. Unpublished data from O'Brien lab showed that keeping Ser315 intact while truncating the last four amino acids of Cx36 C-terminus also caused inversion of the coupling mechanism. This data suggested that PDZ domain binding site at the end of the Cx36 C-terminus also plays a role in regulation. Nagy lab showed that the a number of PDZ domain containing proteins, including ZO-1, ZO-2, ZO-3 and MUPP1, bind directly to the tip of the C-terminal of Cx36 (Li et al., 2004) (Li et al., 2009b) (Li et al., 2012). Phosphorylation of Ser315 and PDZ proteins interaction with the Cx36 C-terminal tip could both contribute to regulation of assembly of a protein complex, that disruption of Cx36 C-terminal could lead to inverted regulation and coupling (Ouyang et al., 2005). In this study we inserted the HaloTag protein into the C-terminus of the connexin, between Ser293 and Ser315, to avoid interference of regular Cx36 activities.

A.
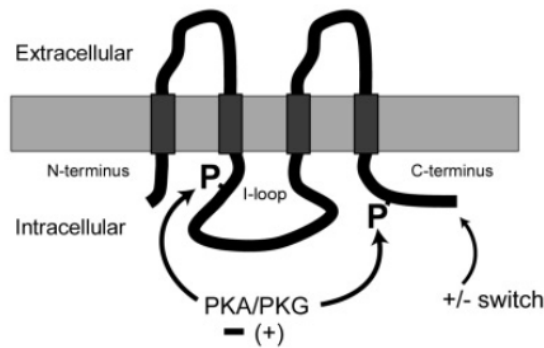
B.
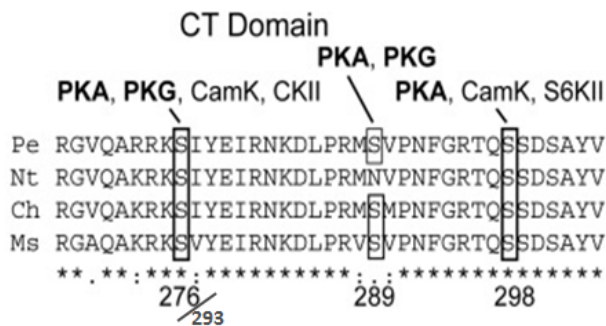
Figure 3. Important regulatory sites in Cx36. A) Ribbon structure of Cx36 showing phosphorylation sites Ser110 and Ser293. B) Cx36 C-terminus structure showing regulatory phosphorylation sites. From Kothmann et al., 2007 (Originally published in Journal of Neuroscience).

2. Turnover rate of Connexins

The regulation of the biosynthesis and degradation of gap junction protein is an essential element in the control of intercellular communication. Connexins are synthesized and co-translationally inserted into the endoplasmic reticulum (ER) as four trans-membrane integral membrane proteins. They are post-translationally assembled into hexamers, known as hemichannels or connexons. The hemichannels insert themselves into the plasma membrane and form functional gap junctions with hemichannels from the adjacent cells (Ahmad et al., 1999b) (Thomas et al., 2005) (Zhang et al., 1996). Assembly of connexins

into gap junctions usually involves the traditional ER-Golgi-TGN-plasma membrane pathway. Cx43 and Cx46 oligomerize into connexons in compartments that include the TGN (Koval et al., 1997) (Musil and Goodenough, 1993), while Cx26 and Cx32 oligomerize primarily in the ER (Falk and Gilula, 1998) (Falk et al., 1994) (Falk et al., 1997). Delivery of new connexin to the plasma membrane is prevented when ER-Golgi transport is blocked by Brefeldin A (BFA) treatment. However, there are reports suggesting that Cx26 can bypass Golgi and directly insert into plasma membrane (Ahmad and Evans, 2002) (George et al., 1998) (Evans et al., 1999) (George et al., 1999) (Martin et al., 2001).

Turnover rates of connexins are exceptionally high. Connexin half-lives reported in the literature range from 1 to 10 hours, with one exception in lens cells (Table 1) (Herve et al., 2007).

Table 1 Comparison of the half-lives reported for different Cxs (or modified Cxs)

Cx	Modified Cx	Half-lives (h)	Cells or tissues[a]	Reference
Cx26		5	Adult mouse hepatocytes	Fallon & Goodenough, 1981
		1.3–2	Cultured mouse hepatocytes	Traub et al., 1989
Cx31		4.1	HeLa cells	Diestel et al., 2004
		6	*HeLa cells*	He et al., 2005
Cx32		4–6	Rat hepatocytes	Traub et al., 1983
		2.5–3	Mouse embryo hepatocytes	Traub et al., 1987
		~3	PC12 cells	VanSlyke et al., 2000
	Cx32T-GFP	3.3	*Hepatocellular carcinoma-derived PLC cells*	Windoffer et al., 2000
	Flagged Cx37	3	*BWEM cells*	Larson et al., 2000
Cx43		1.5–2	*Mouse sarcoma 180 cells and fibroblasts L929*	
		1.5	Chick lens epithelial cells in culture	Musil et al., 1990
		2–2.5	Normal rat kidney (NRK) cells	
		3.1	Novikoff hepatoma cells	Lampe, 1994
		~1.5	BICR-M1Rk cells	Laird et al., 1995
		2.5	E36 Chinese hamster ovary cells	Laing & Beyer, 1995
		3.27	Bovine aortic endothelial cells in culture	Larson et al., 1997
		2.7	Cultured leptomeningeal cells of newborn rat	Hertzberg et al., 2000
		2.66 ± 0.66 to 3.95 ± 0.88	MC3T3 osteoblastic cells	Yamaguchi & Ma, 2003
		2	SK-HEP-1 cells	Thomas et al., 2003
		~1	*BWEM cells*	Laing et al., 1997
		2.3	Bovine retinal endothelial cells	Fernandes et al., 2004
		1–2	Newborn rat cardiac myocytes	Laird et al., 1991
		1.9	Newborn rat cardiac myocytes	Darrow et al., 1995
		1.4	Newborn rat cardiac myocytes	Laing et al., 1998
		1.3	Adult rat heart	Beardslee et al., 1998
	Cx43-GFP	2–3	*HeLa cells*	Hunter et al., 2005
Cx45		4.2	*HeLa cells*	Hertlein et al., 1998
		2.9	Newborn rat cardiac myocytes	Darrow et al., 1995
Cx45.6		2.5	Lens of embryonic chicken in culture	Yin et al., 2000
	Cx49-GFP	10	*HeLa cells*	Breidert et al., 2005
Cx56		2–3 (1st pool)	Chicken lens cultured cells	Berthoud et al., 1999
		48 (2nd pool)		

Cx32T-GFP is a carboxy-terminally truncated version of rat Cx32 and enhanced-GFP chimera

[a] Roman characters, cells where Cx was endogenously expressed; italics, cells where Cx was exogenously expressed, surexpressed or mutated

(From Herve et al., 2007, originally published in Journal of Membrane Biology)

The summarized literature in table 1 addressed mostly non-neuronal gap junction proteins (except Cx45). There was no literature studying the turnover rate of the predominant neuronal gap junction protein, Cx36, until one recent manuscript from the Pereda group (Flores et al., 2012). The Pereda group studied the connection between gap junction turnover and electrical synaptic strength for the first time in goldfish Mauthner cells. Mauthner cells are motor neurons that possess both chemical and electrical synapses.

These synapses are large myelinated club endings (CEs) that belong to auditory afferents that synapse onto Mauthner cells (Figure 4A). The Pereda lab showed ultrastructural evidence that supported the theory that connexin channels are added and removed from the gap junction simultaneously. New connexons are inserted outside of the preexisting gap junction as unpaired gap junction hemichannels, and removed from the gap junction plaque as annular junctions, i.e. double membrane vesicles formed by paired connexons (Figure 4B) (Flores et al., 2012).
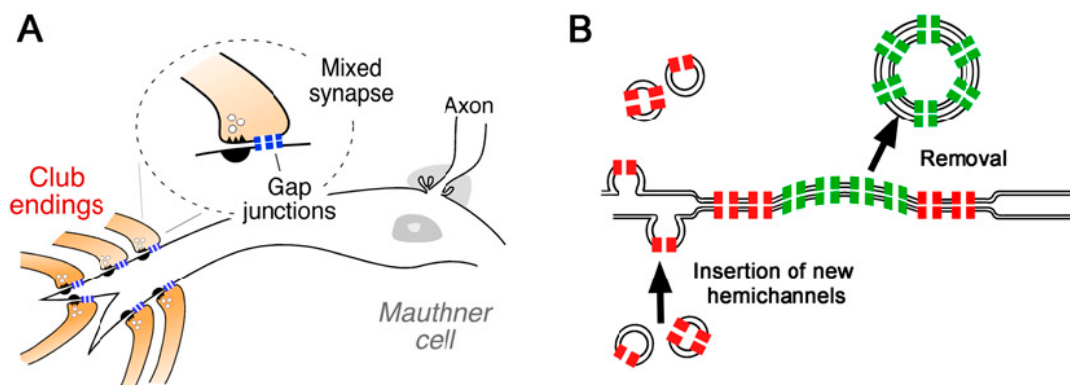
Figure 4: Mauthner cell CEs. A) CEs have a mixture of chemical and electrical synapses on the lateral dendrites. B) Trafficking and turnover of gap junction channels. From Flores et al., 2012 (Originally published in PNAS).

The Pereda lab also used peptides to interfere with exocytosis and endocytosis of gap junction protein. They measured the peptides' effects on the electrical (gap junction mediated) and glutamatergic (chemical synapses mediated) components of the mixed excitatory postsynaptic potential (mixed EPSP) evoked. The electrical and glutamatergic components are separated in time due to membrane time constant of the Mauthner cell and can be identified and measured unambiguously (Figure 5A). The peptides applied are known to modify the strength of glutamatergic transmission at mammalian synapses.

Measuring the glutamatergic component of the mixed EPSP provided a good positive control for their effects on the electrical component (Figure 5D, 5E). Intradendritic application of the dynamin-inhibitory peptide D-15 (amino acids 828-842 of rat dynamin), which is a proline-rich domain that interferes with endocytosis by interrupting dynamin's interaction with amphiphysin, increased the electrical component of the mixed EPSP (Figure 5B), showing that preventing removal of gap junction protein strengthened electrical transmission within minutes. Similarly, injecting SNAP-25 peptide (amino acids 182-192 of SNAP-25), which interferes with formation of SNARE complex, hence interfering with insertion of new hemichannels, decreased the electrical component of the mixed EPSP (Figure 5C), showing that reduced exocytosis weakened electrical transmission. The group reported a half-life of gap junction channels at CEs of 1-3 hours, which is consistent with previous studies of connexin half-lives shown in Table 1 (Flores et al., 2012).
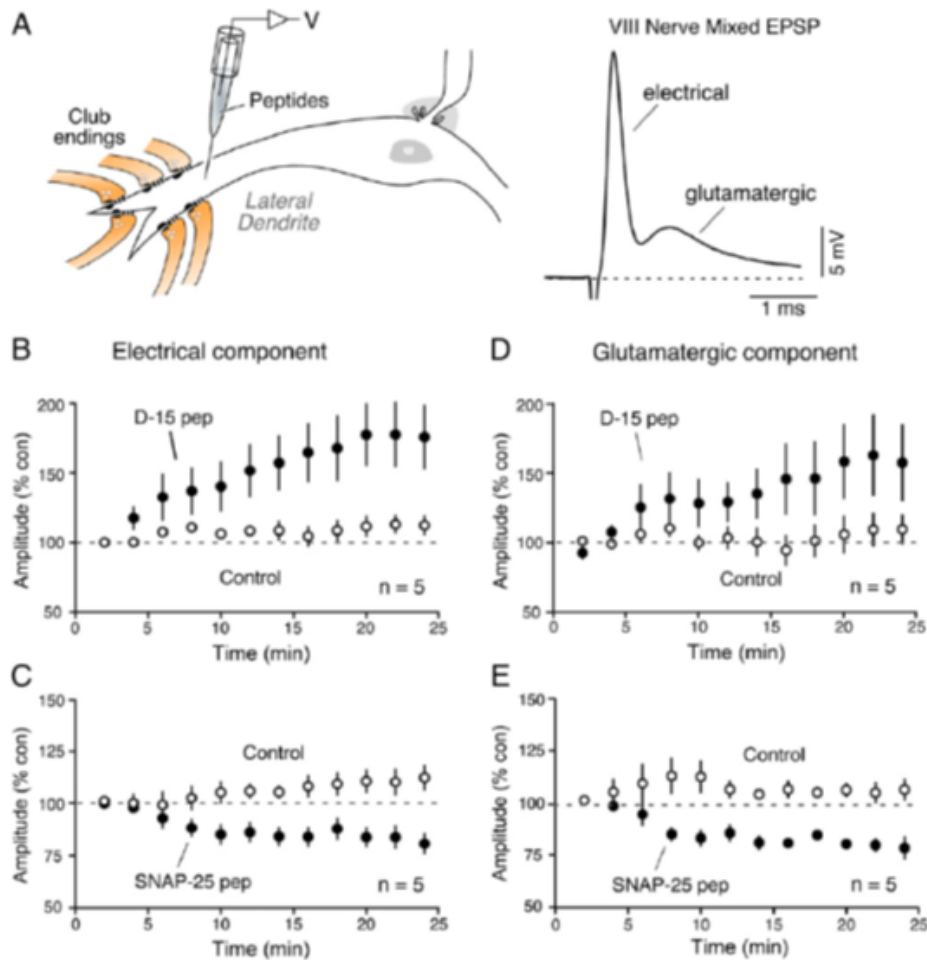
Figure 5: Interfering with endocytosis and exocytosis modifies synaptic strength. A) Experimental apparatus for intradendritic injection of peptides. B, D) D-15 strengthened the electrical transmission as well as chemical transmission. C, E) SNAP-25 pep weakened electrical transmission as well as chemical transmission. From Flores et al., 2012 (Originally published in PNAS).

Most of the turnover rate studies use pulse-chase analysis. A pulse-chase analysis is a method for examining a cellular process occurring over time by successively exposing the cells to a labeled compound (pulse) and then to the same compound in an unlabeled or differently labeled form (chase). Traditional pulse-chase analysis studies use one of the four following methods: metabolic labeling with $[^{14}C]$-bicarbonate (Fallon and Goodenough, 1981), immunofluorescence (Fishman et al., 1995), $[^{35}S]$-labeling (Musil et al., 2000), and

FlAsH (Fluorescein arsenical helix binder) (Gaietta et al., 2002). These methods require the usage of radioactive elements, or use time consuming procedures that require specialized training. In the recent study of electrical synapse turnover rate in Mauthner cells, the turnover rate was assessed by measuring response time of electrical transmission after SNAP-25 and CT-peptide injections. This method presents its own problem due to the susceptibility of the peptides to the actions of peptidases and diffusion from the injection site (Flores et al., 2012). In order to study turnover rate of gap junction in electrical synapses, we need to find a better way to label the connexin, as well as an efficient way to measure and quantify gap junction protein at a particular time point.

3. HaloTag Technology

The ability to label protein efficiently and specifically is very important in studying intracellular protein interactions. Traditional approaches in studying protein interaction include biochemical analysis, cell based analysis, and in vivo models. A variety of methods have been employed for protein interaction studies, such as using antibodies to target endogenous proteins, creating affinity tags to pull down proteins, or attaching florescent proteins to protein of interest for imaging. These methods, however, can be time consuming, or only cover a small spectrum of the study of protein interactions. HaloTag fusion protein provides a new approach to specifically label a protein of interest, and it is applicable to all the approaches in protein analysis.

HaloTag protein is a 34kDa monomeric protein. It is derived from a prokaryotic hydrolase which is not endogenous in eukaryotic cells, allowing high specificity (Georgyi V. Los, 2005). It can be used to generate either N- or C-terminal fusion that can be efficiently

expressed in a variety of cell types. It is genetically engineered to form a covalent bond

with specific, synthetic HaloTag ligands (Figure 6A). The HaloTag ligands are

chloroalkanes that are modified to carry a variety of functional chemical tags for different

types of studies (Los et al., 2008) (Los and Wood, 2007). In this study, we used two cell

permeable HaloTag fluorescent ligands, Oregon Green (OG) and tetramethylrhodamine

(TMR), to label Cx36-HaloTag fusion protein (Figure 6B) (G. Los, 2006).

A.
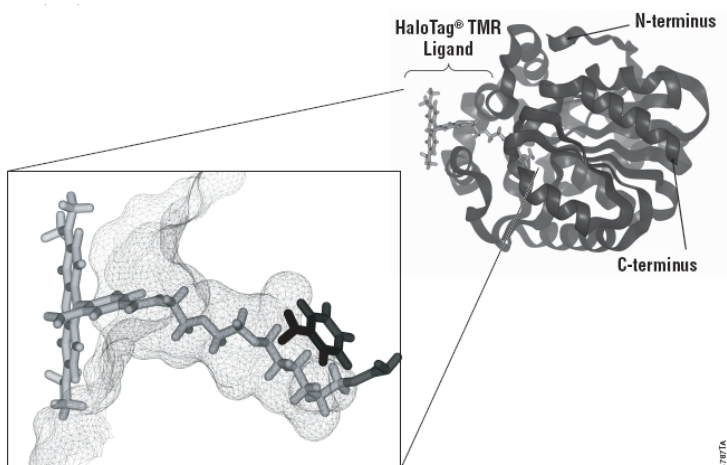
B.
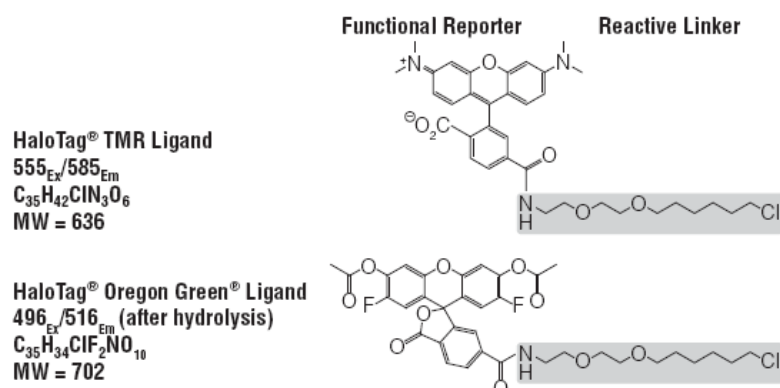
Figure 6: HaloTag technology. A) Ribbon structure of HaloTag protein, the enlarged picture
shows the active binding site between HaloTag protein and HaloTag TMR ligand. B) Structure of
HaloTag TMR ligand and HaloTag Oregon Green Ligand. Originally published on Promega website
(Images reproduced with permission from Promega Corporation).

To this date, very limited studies have investigated the link between Cx36 turnover rate and electrical synapse plasticity. We wanted to see whether the HaloTag technology mentioned above can be used as a new tool for more specific and efficient labeling of Cx36, and is going to be beneficial in future turnover rate studies. In this study, we created a construct of Cx36 and HaloTag fusion protein and used this fusion protein to study Cx36 turnover rate in HeLa cells. We also examined the possible delivery and removal mechanisms of Cx36. We hope by establishing that HaloTag technology can be a useful tool for Cx36 turnover rate study, we can provide insight on how the turnover rate participates in regulating electrical synapse plasticity.

Materials and Methods:

Cells and Reagents

All media, fetal bovine serum and cell culture reagents were obtained from Invitrogen (Grand Island, NY). HeLa cells were obtained from American Type Culture Collection (Rockville, MD, Cat#CCL-2). HeLa cells were grown in complete MEM supplemented with 10% fetal bovine serum, 1% antibiotic-antimycotic (Penicillin/Streptomycin/amphotericin B). Transfection of HeLa cells was performed with GenePORTER® 2 transfection reagent kit from Genlantis (San Diego, CA). PKA activator, Sp-8-cpt-cAMPS and PKA inhibitor, Rp-8-cpt-cAMPS, were from Alexis (San Diego, CA). HaloTag vector, HaloTag ligands Oregon Green (OG) and tetramethylrhodamine (TMR) were purchased from Promega (Madison, WI), and Brefeldin A was purchased from Cell Signaling Technology (Danvers, MA).

Creating Cx36-HaloTag construct and transfection

The HaloTag open reading frame was inserted into an internal site in the C-terminus of Cx36 using Cold Fusion cloning kit. The location of the insertion we chose would not disrupt the regulatory C-terminal phosphorylation sites nor block the C-terminal PDZ interaction motif (see Figure 9).

HeLa cells were plated on 12mm cover glasses and grown to 75% confluence overnight in 35mm culture dishes. HeLa cells were transiently transfected using GenePORTER® 2. We used 1.5μg of GenePORTER® 2 and 2μg of Cx36-Halo plasmid DNA per 35mm culture dish. All the following experiments were conducted 24 hours after transfection.

Tracer coupling

Transfected HeLa cell cover glasses were maintained in Ringer's medium supplemented with 0.05% Neurobiotin. Cells were scraped with a 25-gauge needle. Incubation was done at 25°C in the oxygenated medium with Neurobiotin for 10 minutes to allow loading and diffusion. Cells were then fixed with 4% paraformaldehyde (in PBS with 0.5% Triton X-100 and 0.1% NaN3, pH7.4) after two washes to remove excess Neurobiotin. PKA activator and inhibitor were added to the oxygenated incubation medium at the beginning of the incubation period. Cells were then visualized with streptavidin-Cy3 (Jackson ImmunoResearch, West Grove, PA), and photographed on a Zeiss fluorescence microscope using Simple PCI software (Compix, Cranberry Township, PA). The diffusion coefficient of the coupled HeLa cells was calculated by measuring the fluorescence intensity of the cells (O'Brien et al., 2004)(Figure 7).

The analysis utilizes a linear 25-compartment diffusion model of the type described by (Zimmerman and Rose, 1985) to fit the Neurobiotin concentration and diffusion distance data. This model has been applied to neural networks to assess gap junction coupling in the retina (Mills and Massey, 1998) (O'Brien et al., 2004) (Li et al., 2009a). In this model, the compartments are defined as individual cells, and the major parameter that governs diffusion of Neurobiotin is the diffusion coefficient through gap junctions between two adjacent cells (Figure 7A). The movement of tracer, i.e. Neurobiotin, between adjacent compartments is described by a series of 25 differential equations that are solved for tracer flux given the total amount of diffusion time and a diffusion coefficient, k. The diffusion coefficient k represents the proportion of tracer that diffuses from the first compartment to the next per second. The diffusion coefficient k will be a value between 0 and 1, and all values larger

than 0 represent measurable amount of tracer diffused, hence the presence of gap junction coupling.

Optimal fitting of intensity data to the model was determined in MatLab (Mathworks, Natick, MA) by varying the diffusion coefficient k and another parameter, bo, the bolus loading rate. The parameter bo was defined as the rate of addition of tracer to the initial compartment for the loading period, which was assumed to be 1 minute in the scrape-loading experiments, and was set to zero thereafter. The value of the parameter bo was determined by the total amount of tracer in all the compartments and is not affected by the diffusion coefficient between adjacent cells. Data fits were determined by plotting cell intensities on a log intensity axis and determining the diffusion coefficient k that best fit the rate of decline of cell intensity with distance from cell of origin, and the rate of delivery, bo, that fit the overall tracer concentration (Figure 7B). The effect of varying bo was only to translate the position of the curve vertically on the log intensity axis (data not shown). It was not affected by and has no effect on the diffusion coefficient k (Mills and Massey, 1998) (O'Brien et al., 2004) (Ouyang et al., 2005) (Li et al., 2009a). Diffusion coefficients were compared under different drug treatment conditions using t-test.

A.
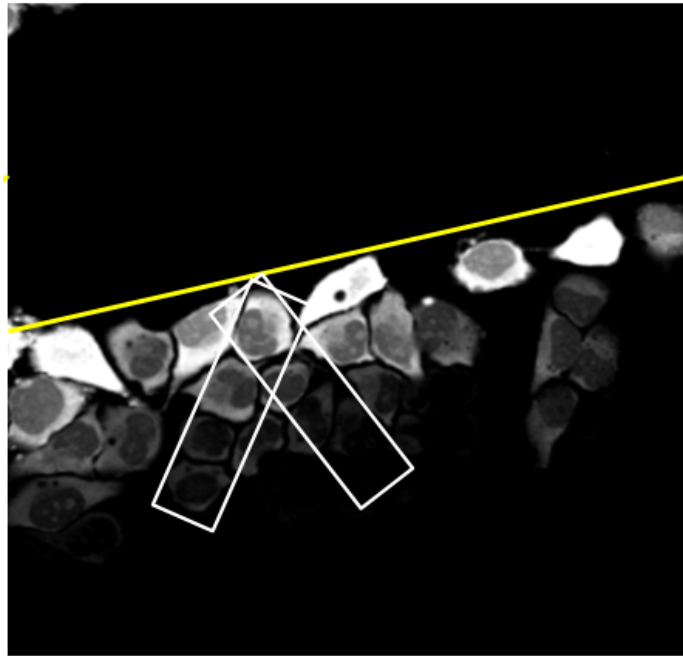
B.
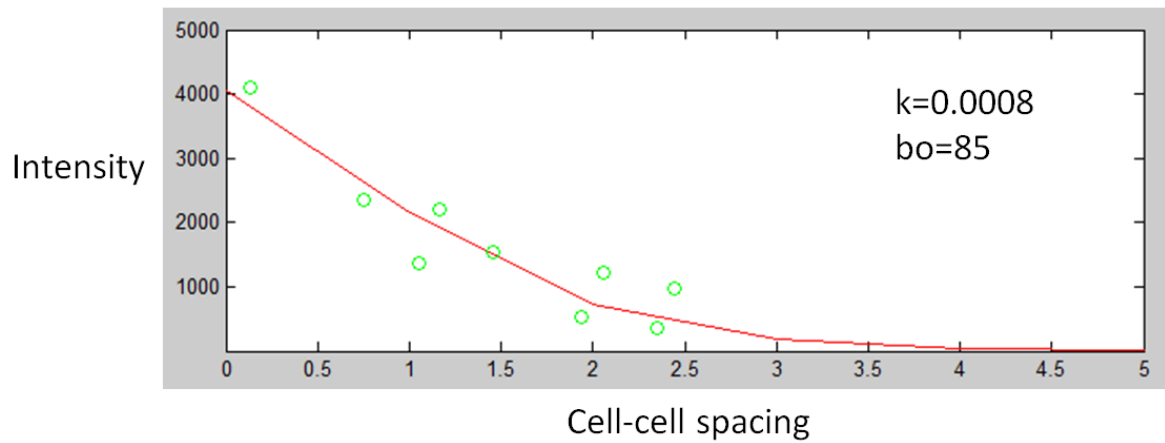
Figure 7. Scrape-loading analysis. A) Picking compartments. In this experiment, compartment represents one HeLa cell that is coupled to two neighbors in a linear array via a coupling resistance (a gap junction) characterized by the diffusion coefficient. B) Intensity data are plotted vs. distance from the cut edge in cell-to-cell spacing (mean of spacing measured from the same image). The data are fit to the model by systematic adjustment of the k (diffusion coefficient) and bo (tracer loading rate into the initial compartment at the cut edge) parameters. Diffusion time for the model is set by the actual time from cutting to fixation of the sample (16 minutes in this experiment).

Imaging: Live cell imaging, fixed cell imaging and immunolabeling

Transfected HeLa cell cover glasses were incubated in Ringer's medium containing 5µM HaloTag TMR fluorescent ligand for 15 minutes. Cover glasses were then washed to remove unbound ligand and transferred to a microscope to capture images.

After live cell imaging, cells were fixed in Ringer's medium with 4% paraformaldehyde for 10 minutes. Cover glasses were then incubated in PBST with 10% donkey serum to block non-specific binding. Cover glasses were incubated overnight at 4°C with Cx36 primary antibody in PBST with 10% donkey serum followed by fluorescent secondary antibody in 5% donkey serum for 3 hours. Cover glasses were then washed, mounted and transferred to a confocal microscope to capture image. HaloTag TMR was visualized with the TRITC filter set, and the Cx36 was visualized with the Cy5 filter set. Images of HeLa cells were digitally captured using a Zeiss LSM 510 Meta confocal microscope (Thornwood, NY) with similar settings of pinhole, contrast, and brightness parameters.

Pulse-chase analysis

Transfected HeLa cell cover glasses were incubated in Ringer's medium containing 5µM pulse labeling ligand Oregon Green (OG) for 15 minutes in a 24-well plate in 37 degree incubator. Cover glasses were then washed to remove unbound ligand and incubated with Ringer's medium at 37 degrees, and were labeled with tetramethylrhodamine (TMR) HaloTag ligand at various times (0.3, 1, 2, 3, 4, and 5 hours after pulse labeling) for 15 minutes. All cover glasses were fixed with 4% paraformaldehyde, and transferred to a

confocal microscope for image capturing. HaloTag TMR was visualized with the TRITC filter set, and HaloTag OG was visualized with the FITC filter set.

Images were captured with a Zeiss LSM 510 confocal microscope and analyzed with the same settings using SimplePCI software. Regions of interest (ROIs) were selected by setting an intensity threshold and applying a minimum size threshold. ROIs were defined as contiguous pixels with intensity threshold greater than 20% of the total intensity range, and which covered a minimum area of 200 pixels. Each image was then manually scanned for individual ROIs that fit in the criteria but were not part of the gap junction plaques. They were manually removed from the analysis (Figure 8A). Mean and total fluorescent intensity was measured in each channel for each ROI (Figure 8B). At any given time point, the amount of pulse labeling present is defined as the percentage of the total of pulse labeling over total labeling (pulse + chase). The half-life of Cx36 was calculated by fitting an exponential curve to the percentage of pulse labeling over time.

A.
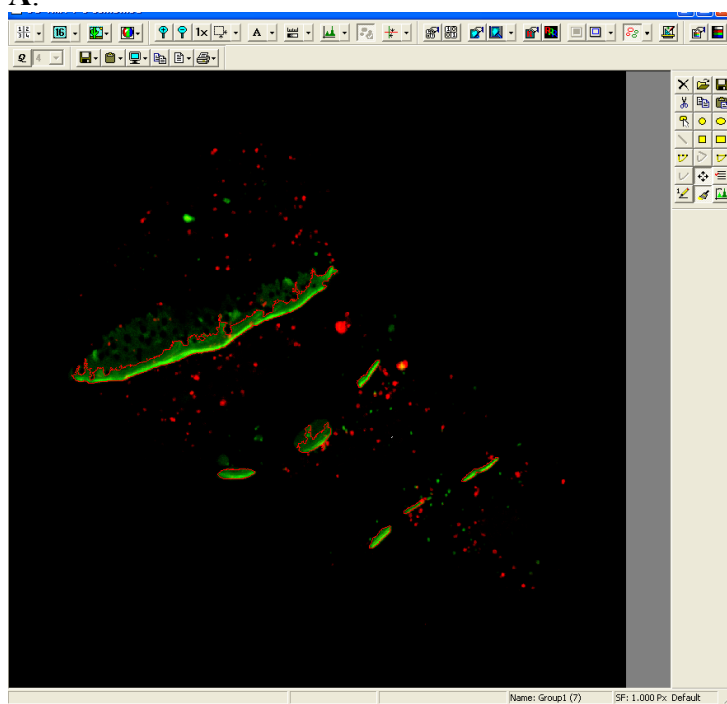
B.
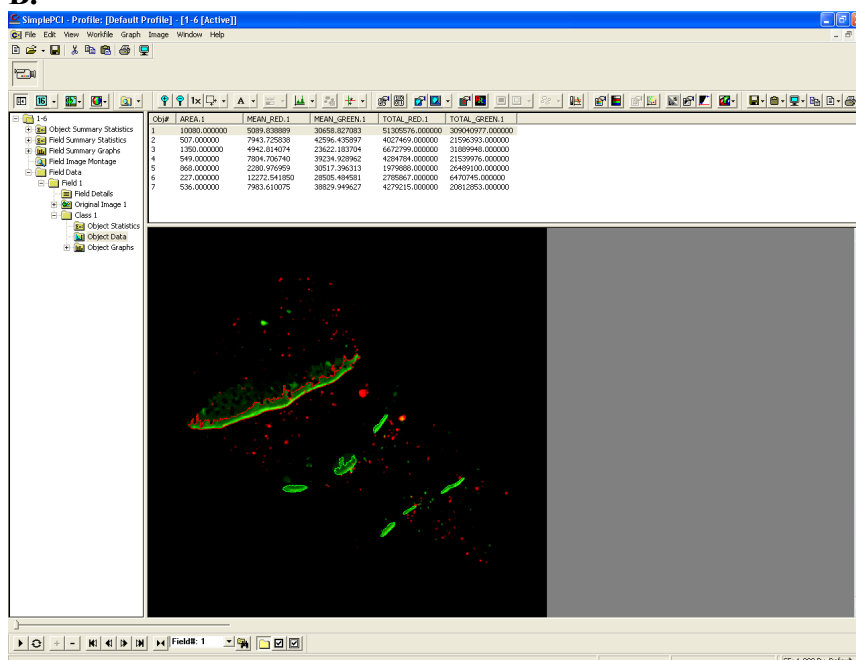
Figure 8. Pulse-chase experiment data collecting with SimplePCI. A) Choose the ROIs by setting a size (200 pixels) and intensity (20% of maximum intensity) threshold. Areas selected that did not represent gap junction plaques were manually removed from the data pool. B) Mean and total fluorescent intensity for both the TMR channel and OG channel were measured in each ROI.

Drug Treatment: BFA

To analyze the transport of Cx36 from ER to the PM, transfected HeLa cells were treated with BFA (2µg/ml) during the pulse-chase analysis. BFA was added to the cells after 15 minutes of pulse label OG incubation and washing, and was left in the wells before the chase label TMR was added. Cells were incubated in TMR for 15 minutes. In the control experiment, cover glasses were treated with DMSO (2µg/ml) and the treatment was identical to that of BFA.

Results

1. Cx36-HaloTag fusion protein can form functional Cx36 gap junction in HeLa cells. The gap junctions formed are regulated by PKA activity like the wild-type.

To study Cx36 without interfering with its protein-protein interactions, we had to carefully choose a site to insert the HaloTag open reading frame where it is not close to the functional or regulatory amino acids. The insertion site was in the internal site of the C-terminus of Cx36, between the two important serine sites (S293 and S315) (Figure 9).

A.

Cx35 CT   RGVQARRKSIYEIRNKDL ▷ **HaloTag** ◁ PRMSVPNFGRTQSSDSAYV

B.
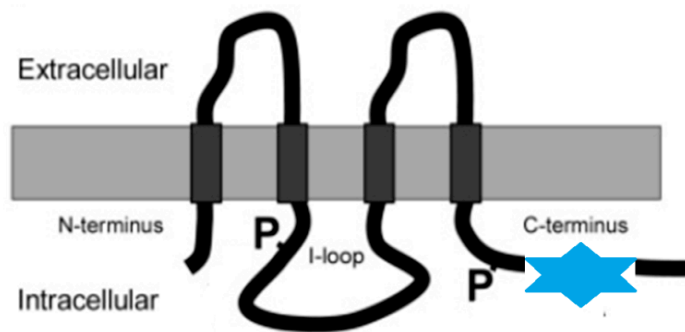
**Figure 9. Insertion of HaloTag vector into Cx36 C-terminus.** A) Sequence of perch Cx35 C-terminal indicating the insertion point of HaloTag open reading frame. Red arrows indicate regulatory serines (S276 and S298). B) Ribbon structure of Cx35 showing relative location of HaloTag.

To determine if Cx36-Halo construct can form gap junctions properly in HeLa cells, we transfected HeLa cells with Cx36-Halo construct, and labeled the cover slips with HaloTag TMR ligand 24 and 48 hours after transfection. To better determine the efficiency of the TMR ligand, we labeled the Cx36-Halo construct at 0.5x, 1x, and 1.5x the concentration of the 1x TMR ligand working solution. After labeling, we transferred the cover slips on a microscope for live cell imaging. We can see that Cx36 gap junction 24 hours after transfection with Cx36-Halo construct (Figure 10a-c). In the 24 hour after transfection images, we can see that Cx36-Halo transfected HeLa cells have successfully formed gap junctions with one another; the concentration of TMR ligand did not have a noticeable effect on the labeling of gap junction. In the 48 hour after transfection images, we can still find gap junctions (Figure 10d-f). There are also many brightly labeled clusters inside the cells, suggesting internalization of Cx36-Halo protein is common 48 hours after transfection. To achieve the best result in labeling Cx36-Halo in HeLa cells, we transfect HeLa cells with Cx36-Halo construct for 24 hours, and label them with 1x TMR ligand working solution for all the future experiments.
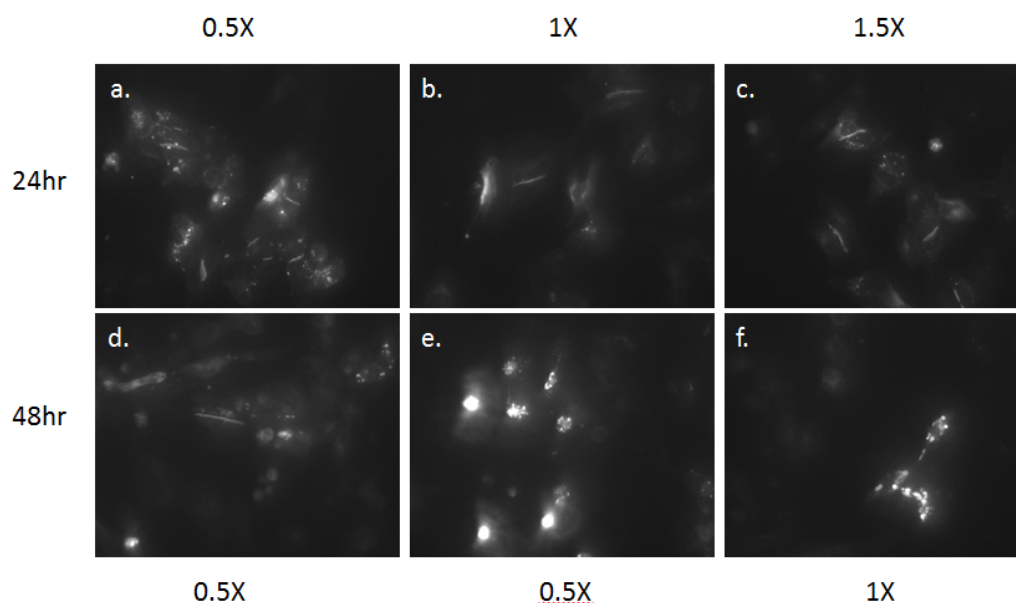
Figure 10. Live cell imaging of HeLa cells transfected with Cx36-Halo structure. (a-c) are images 24 hours after transfection. (d-f) are images 48 hours after transfection. (a,d), (b,e), (c,f) are labeled with 0.5x, 1x, 1.5x the concentration of TMR ligand working solution.

In order to confirm that the gap junctions we observed were formed by Cx36, we co-labeled the cover slips with Cx36 antibody. The gap junctions that showed HaloTag TMR labeling were positively labeled with Cx36 antibody (Figure 11), confirming that TMR labeling is efficient and sufficient in labeling Cx36 gap junctions in transfected HeLa cells.
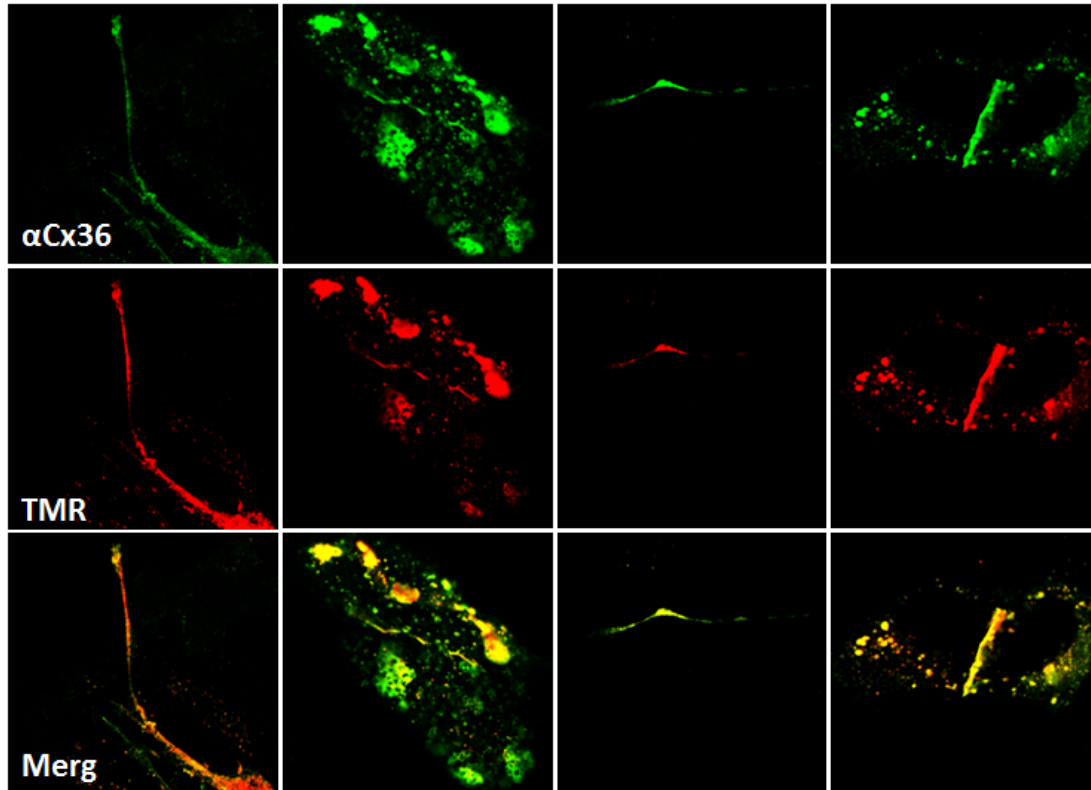
Figure 11. Fixed cell imaging of HeLa cells double labeled with Cx36 primary antibody and TMR ligand.

In previous studies, we established that Cx36 coupling is regulated by PKA activity. In order to see whether introducing the HaloTag protein to Cx36 caused any functional changes in Cx36 regulation, we performed scrape-loading experiments using HeLa cells transiently transfected with Cx36-Halo construct. We observed similar regulation as the ones transiently transfected with wild-type Cx36 (Figure 12). Treatment of Rp increased coupling significantly, while the treatment of Sp showed no significant changes. Control experiment was performed with HeLa cells transfected with HaloTag protein vector alone (Halo-EV) without Cx36. Altering PKA activity did not change the amount of coupling. We observed coupling in the control experiment as well, presumably from endogenous connexin present in HeLa cells, and it was not regulated by changes in PKA activity.

A.
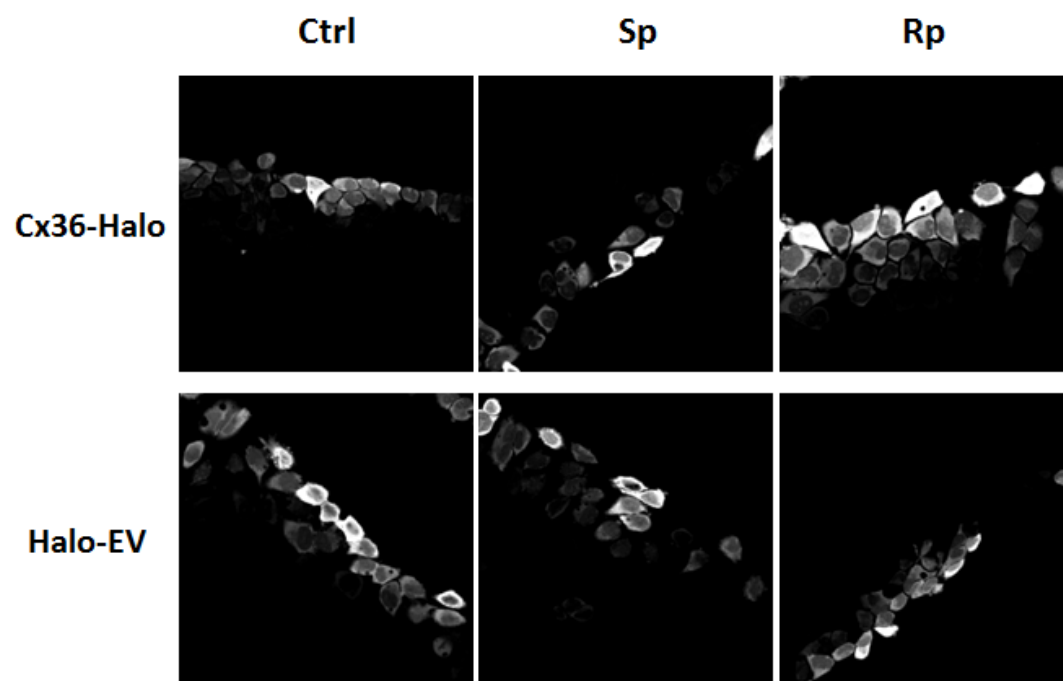
B.
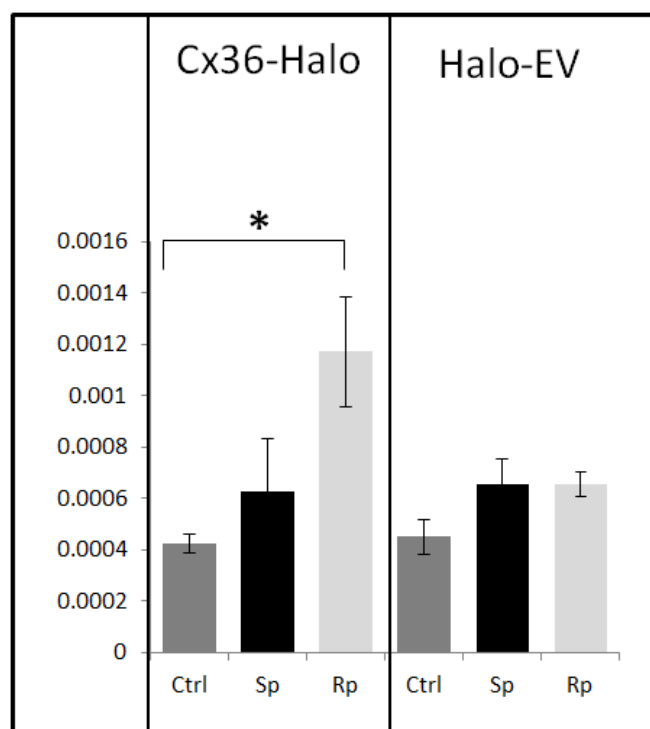
Figure 12. Tracer coupling measurements in HeLa cells transiently transfected with Cx36-Halo construct. Ctrl – control; Sp – 20 μM Sp-8-cpt-cAMPS (PKA activator); Rp – 20 μM Rp-8-cpt-cAMPS (PKA inhibitor). Data are means ± SEM, * P<0.05.

2. Cx36 has a half-life of 2.8 hours in HeLa cells.

To study the turnover rate of Cx36 in HeLa cells, we performed pulse-chase study using two different fluorescent ligands of HaloTag protein. Cover slips that were plated with Cx36-Halo transfected HeLa cells were labeled with HaloTag OG ligand at time 0, and followed by HaloTag TMR labeling at hour 0.3, 1, 2, 3, 4, 5. At 0.3 hours, we can see that the majority of the gap junction was labeled with OG (Figure 13A). As the time progressed, the amount of TMR labeling increased in the gap junction and the amount of OG labeling decreased.
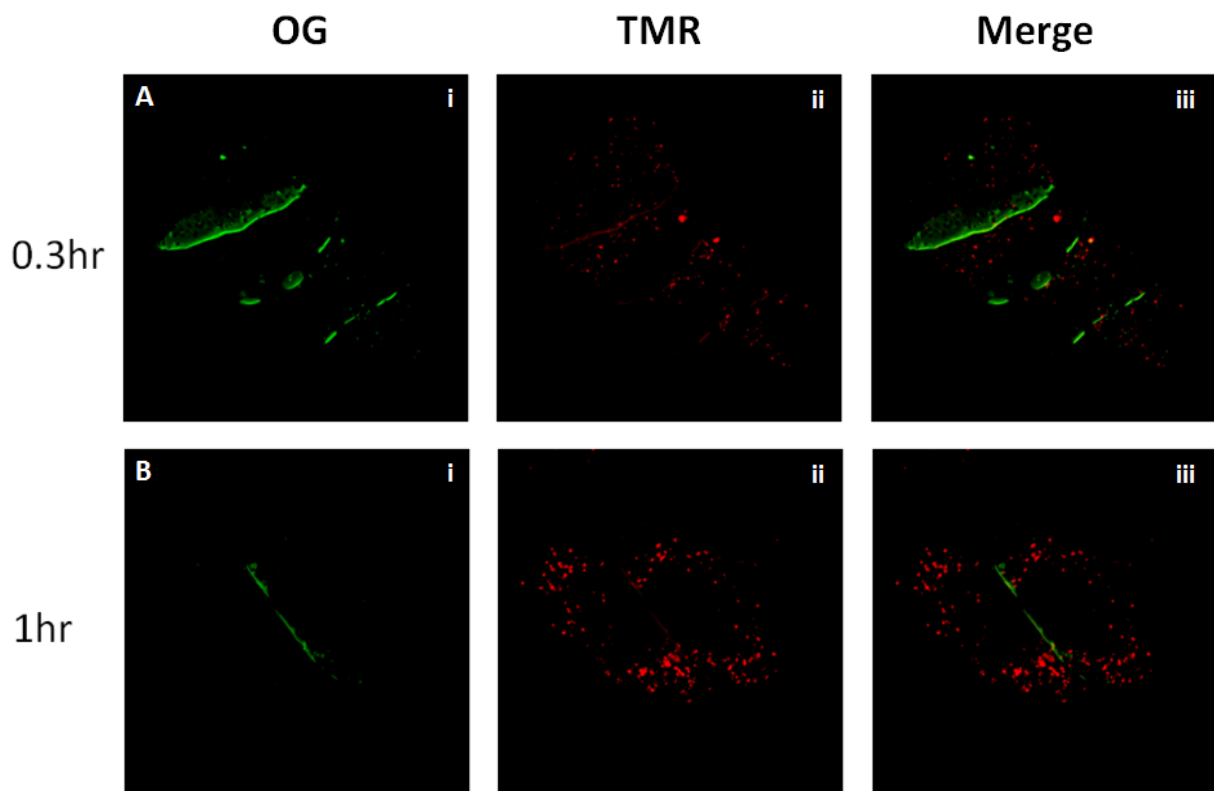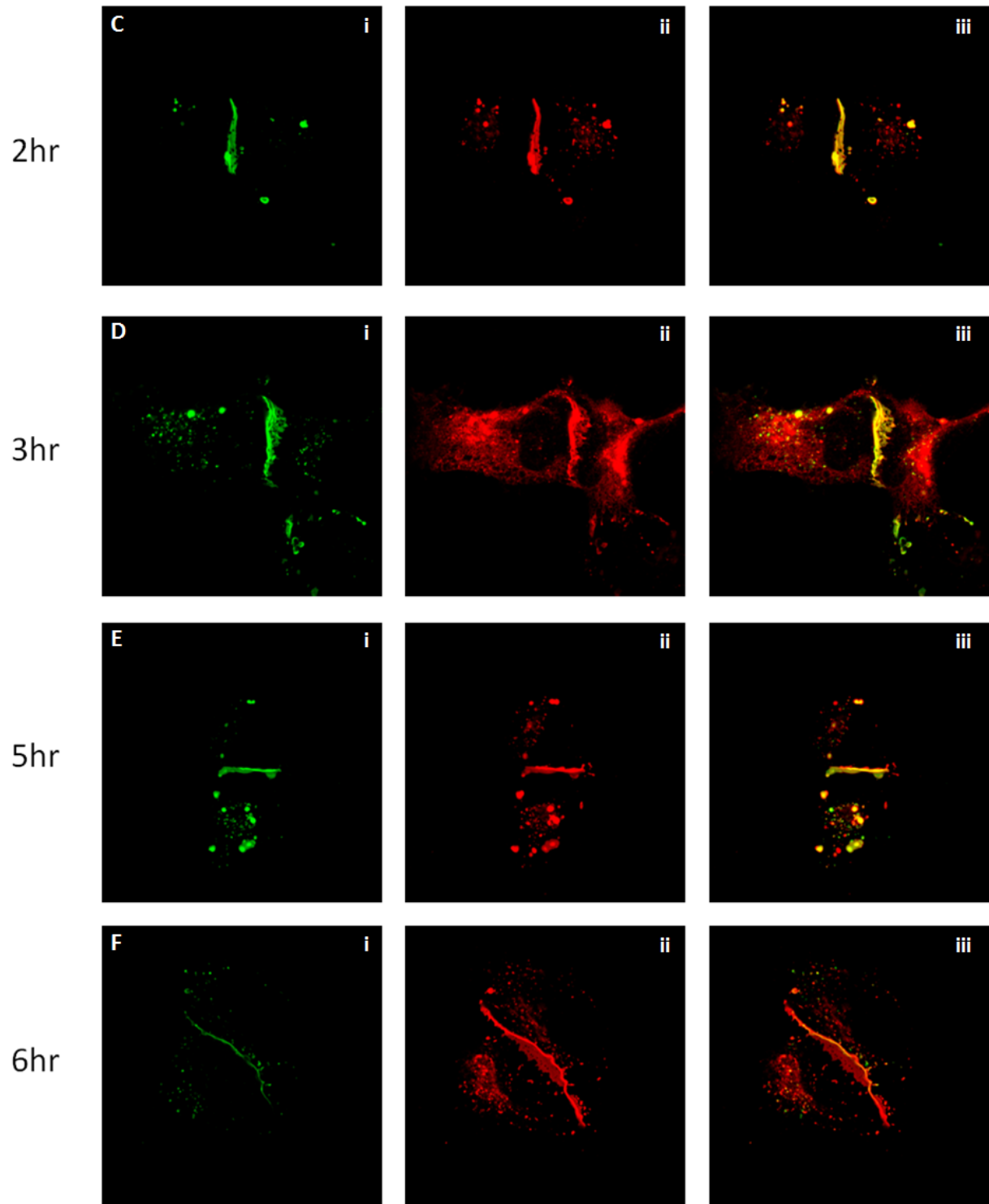
Figure 13. Pulse-chase analysis of Cx36 turnover rate. A-F) confocal microscope images of Cx36-Halo in HeLa cells labeled with OG (pulse) and TMR (chase) at hour 0.3, 1, 2, 3, 5, 6.

In the last time point, the majority of the gap junction was labeled with TMR.   The

TMR label was largely present in small vesicles throughout all the time points, and partially

and increasingly infused into the gap junction (Figure 13Aii-Fii). The TMR label at hour 6

was mixed throughout the whole gap junction (Figure 14), not just on the outer edge as

previously reported (Falk et al., 1994). It showed a progressive removal of the old gap

junction protein, which was labeled with OG, and replacement of new gap junction protein,

which was labeled with TMR.
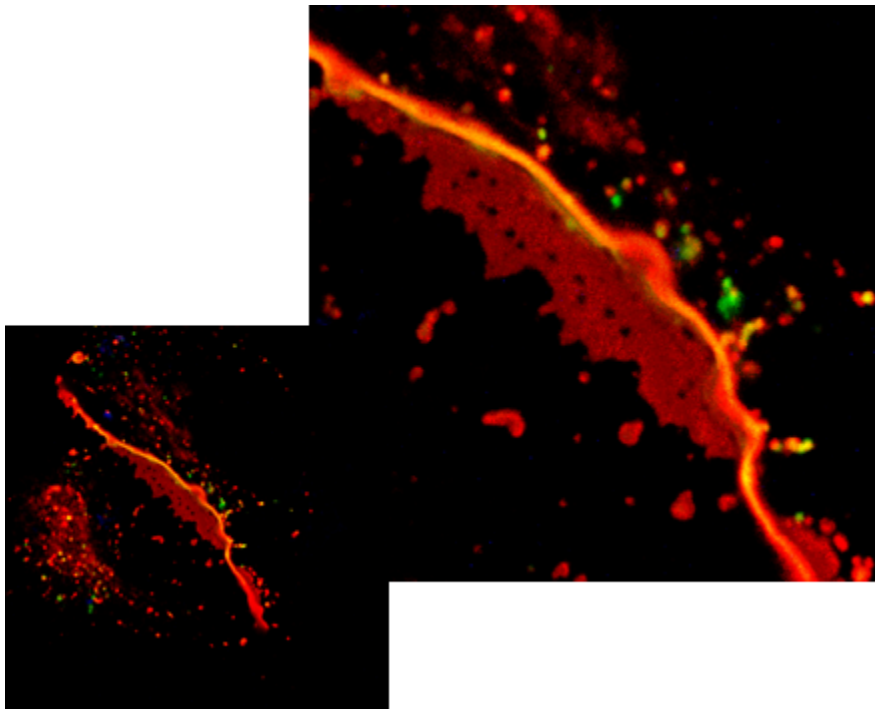
Figure 14. Zoomed in image at hour 6.

We used SimplePCI program to measure the amount of OG and TMR labeling in

each time point, and calculated the percentage of the old gap junction protein in relationship

with the total amount of gap junction protein present (Figure 15). The decay was plot in

exponential curve (we used scatter plot of individual data point to provide a more accurate fit for the curve). The calculated half-life for the decay was 2.8 hours, which is consistent with the previous studies.

$T_{1/2}=(\ln2)/\lambda$
$=(\ln2)/0.246$
$=2.82hrs$

$y = 0.9464e^{-0.246x}$
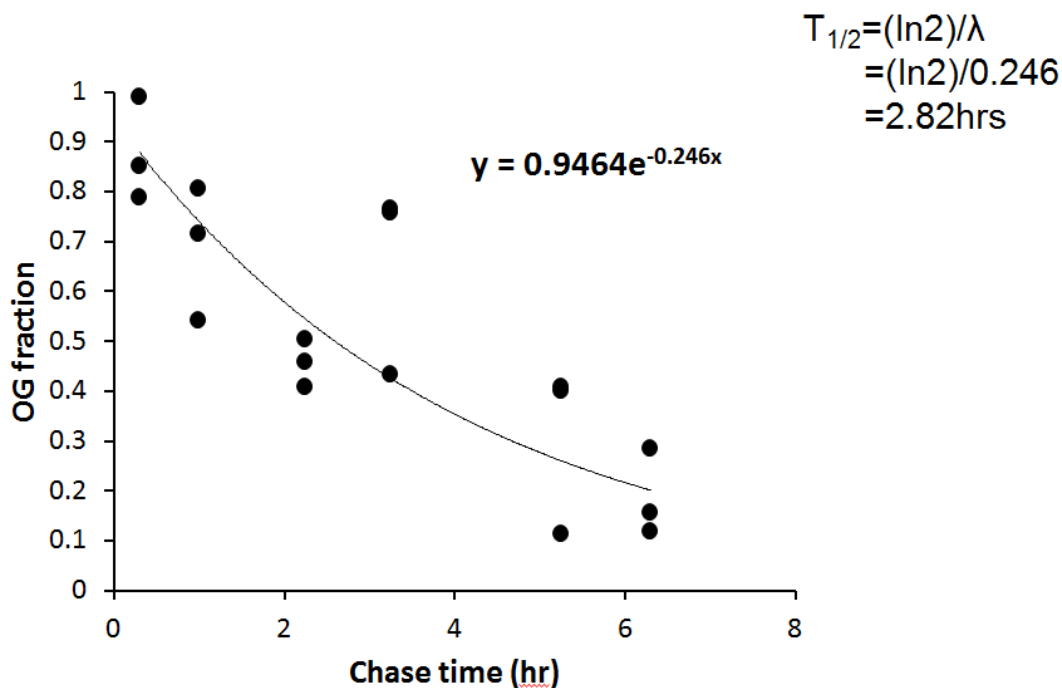
Figure 15. Calculation of Cx36 half-life in HeLa cells. .

3. Treatment of the transfected cells with Brefeldin A successfully blocked the assembly of new gap junction.

With the exception of Cx26 (Zhang et al., 1996), it is generally considered that connexins are modified in the ER (Ahmad et al., 1999a) (Zhang et al., 1996), transported to Golgi, assembled in the TGN (Koval et al., 1997) (Musil and Goodenough, 1993), and finally inserted into the plasma membrane (Laird, 1996; Thomas et al., 2005) (Laird, 1996).

To confirm that the assembly of Cx36 to the plasma membrane involves the same pathway, we repeated the pulse chase analysis with treatment of BFA, which disassembles the Golgi apparatus complex. The original gap junctions were again labeled with OG, and chased with TMR. We saw that at time 0.3 hours, all the gap junctions were labeled with OG, with minimal amount of TMR labeling (Figure 16A). As time progressed, the amount of TMR labeling did not increase in the gap junction. Most of the TMR label was present in small vesicles and some large vesicles; almost none integrated into the gap junctions (Figure 16Aii-Fii). At the 5th hour, the OG was still the only labeling present in the gap junctions (Figure 16F). We concluded that Golgi was essential for Cx36 gap junction assembly.
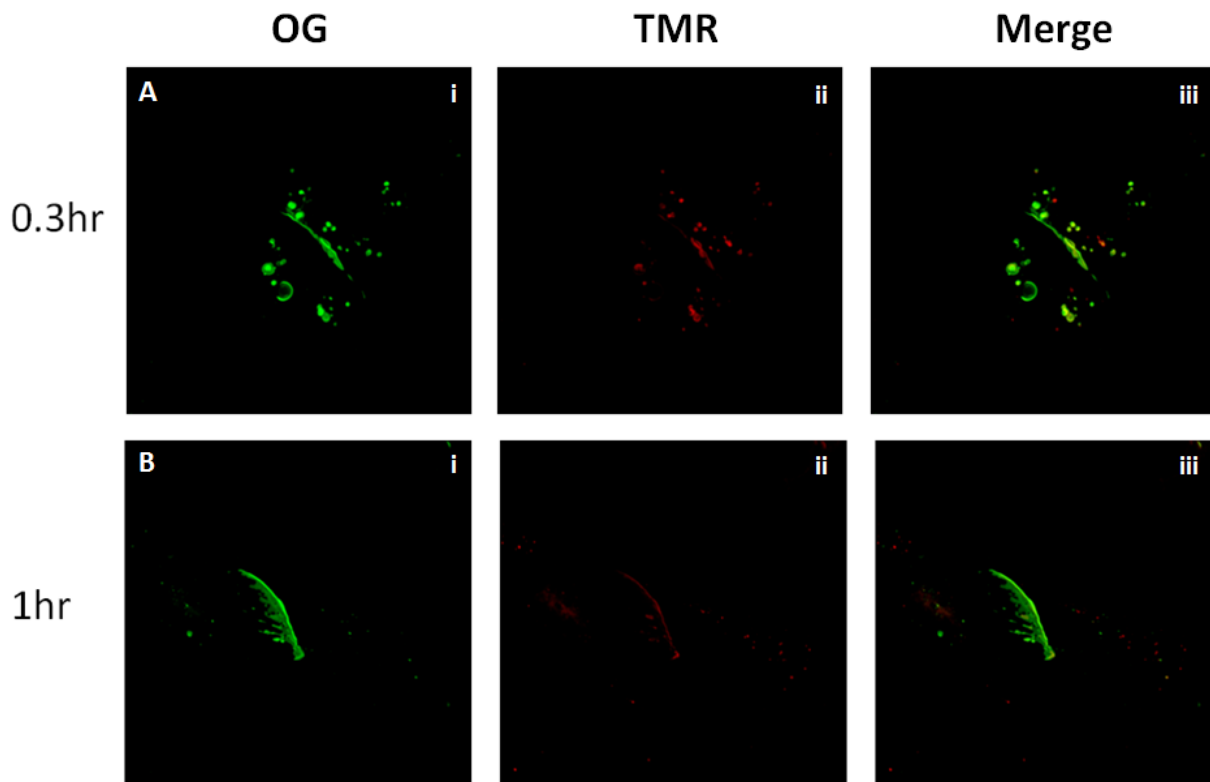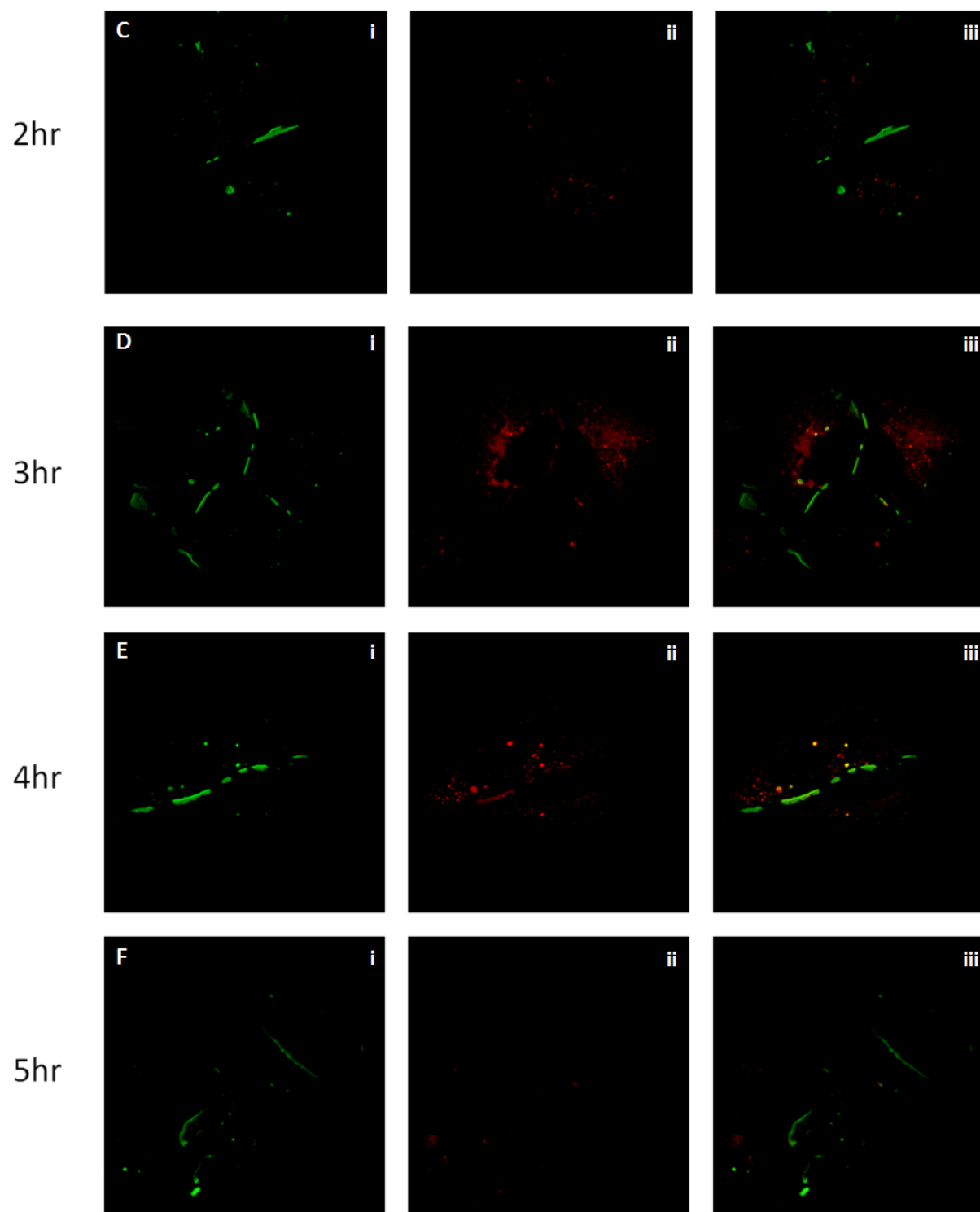
Figure 16. Pulse-chase analysis of Cx36-Halo in HeLa cells with treatment of BFA.

We performed the same SimplePCI analysis to evaluate the fraction of OG labeling throughout the time points. The fraction of OG present in the gap junction showed no significant change from hour 0 to 5 (Figure 17). OG label remained to be the majority of the entire label present in the gap junction. There was a small amount of TMR label present throughout all the time points, probably due to incomplete OG labeling at hour 0.
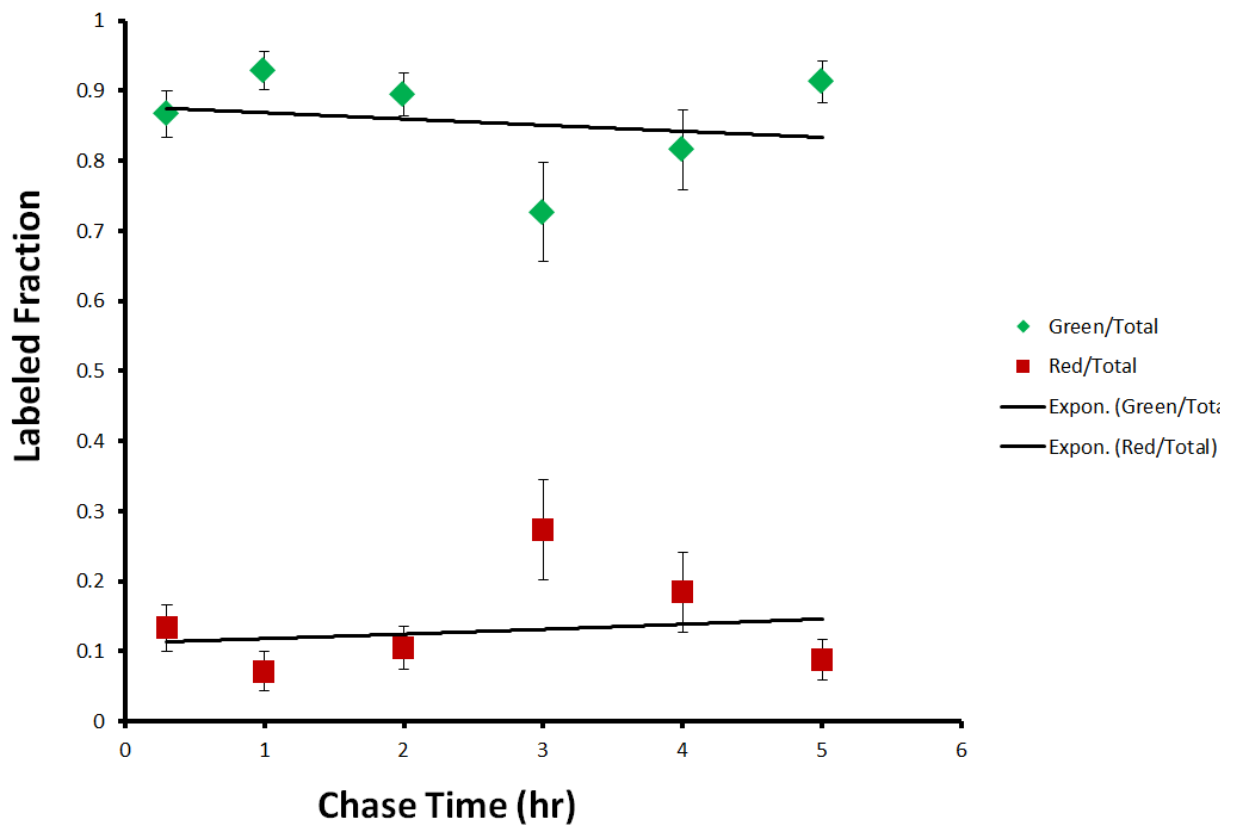
Figure 17. The fraction of OG and TMR labels present throughout the time points.

4. Cx36 is trafficked to the plasma membrane in vesicles, and removed as annular gap junctions

It has been reported that new connexins are trafficked in vesicles as undocked hemichannels and removed as double membrane vesicles called annular junctions (Laird,

1996). In our confocal microscope images, we observed two different types of vesicles close to the gap junctions. These vesicles were present throughout all the time points (Figure 18).
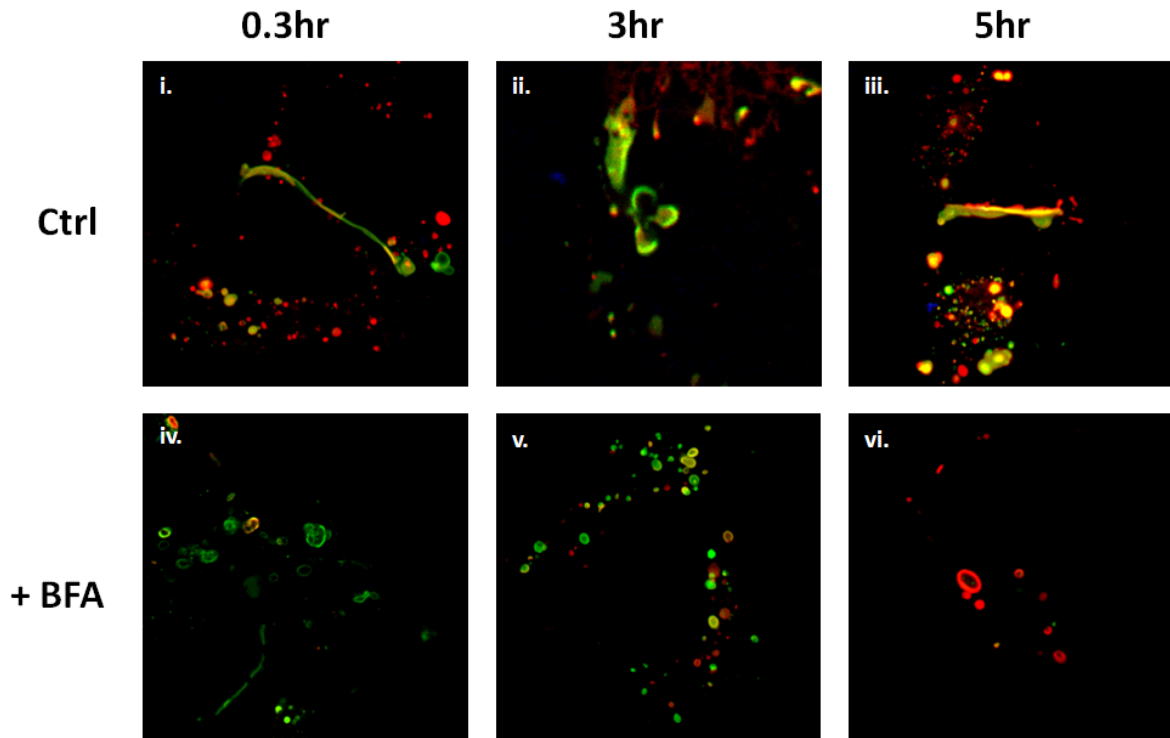
Figure 18. Presence of vesicles throughout all time points in pulse-chase analysis.

The first type of vesicle is small in size and solid. These vesicles were mostly labeled with chase label (TMR). They were often observed on the periphery of the pre-existing gap junction plaques (Figure 19 arrows). In a few scenarios, they were present in the gap in an existing gap junction (Figure 19A yellow arrow). These small vesicles were often found on the end of newly synthesized gap junctions, with a few in the middle section as well (Figure 19B). The second type is significantly larger in size, and these vesicles are usually hollow in the middle. In the HeLa cells with control treatment (Figure 16i-iii), these

vesicles were usually a mixture of OG labeled (Figure 19 solid arrowheads) and TMR

labeled (Figure 19 asterisks). The OG labeled large vesicles were usually close to pre-

existing gap junctions whereas the TMR labeled large vesicles were generally further away

(Figure 19B and C). We also found OG labeled Cx36 budding off the pre-existing gap

junction (Figure 19B blue arrows) near the end as well as in the middle of a gap junction. In

the BFA treated cells (Figure 18iv-vi) where gap junctions are less abundant, we found that

most of the large vesicles were OG labeled in the beginning hour, most of the large vesicles

were TMR labeled in the final hour, and a mixture of both in between. We speculate that

the small vesicles are synthesis vesicles that contain undocked hemichannels that are

transported to the gap junction for exocytotic incorporation. The large ring shaped vesicles

are removal vesicles. They form double membrane annular junction, where connexons are

paired as gap junctions. Usually the removal vesicles would be OG labeled, but we saw

TMR labeled removal vesicles as well. This is probably because Cx36 is synthesized in

excess. As a result, newly synthesized Cx36 proteins get packaged into vesicles to be

removed before ever incorporated into gap junction plaques. In the BFA treated cells, newly

synthesized Cx36 cannot integrate into gap junctions. They still formed large hollow

vesicles that morphologically resemble annular junctions. They are unlikely to be the

conventional annular junctions since these newly synthesized Cx36 never reached the

plasma membrane and docked with hemichannels from the adjacent cells. A previous study

showed that when connnexins are over-expressed, double-membraned gap junctions form

within the intracellular compartment, including the ER (Kumar and Gilula, 1992). These

annular junctions formed by TMR labeled Cx36 double-membraned gap junctions are

probably the artifact of over-expresion of Cx36 in HeLa cells. These annular junctions are

transported to lysosomes subsequently where the gap junction proteins are degraded (Laird, 1996) (Thomas et al., 2002).

A.
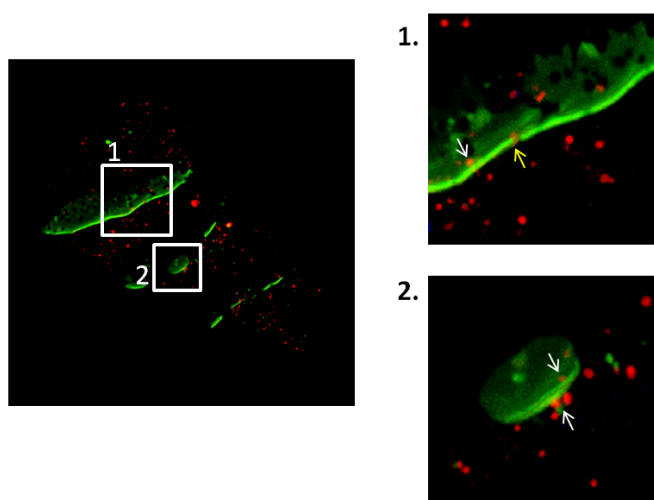
B.
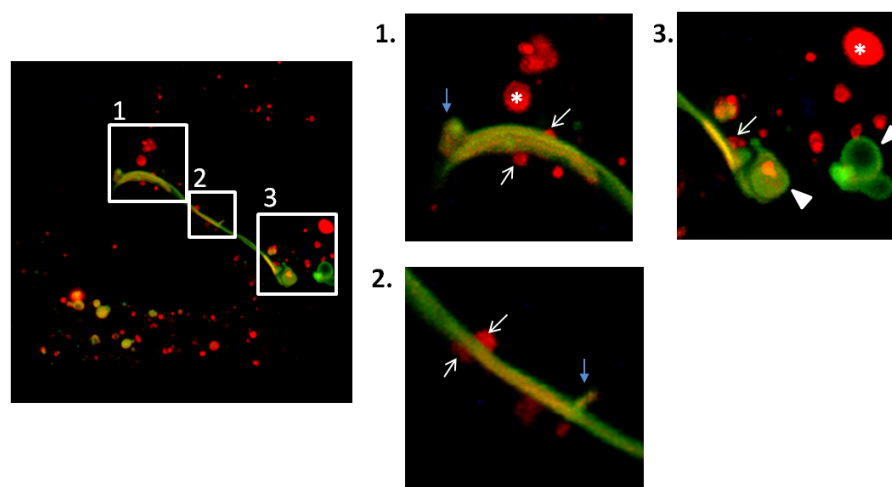
C.
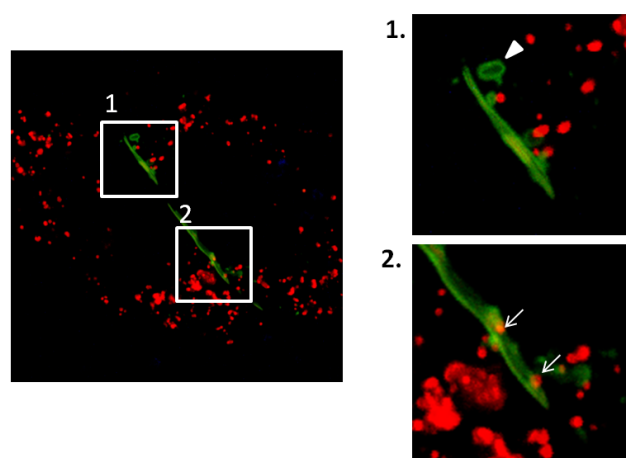
Figure 19. Endocytosis and exocytosis of Cx36 into the gap junction.

Discussion

Gap junction protein turnover

   To study the turnover rate of gap junction protein, it is important to develop a means to label and track gap junction protein efficiently and specifically. In this study, we employed the new HaloTag technology to label Cx36 in HeLa cells. We created one genetic construct inserting HaloTag protein into the C-terminal of Cx36. Our live and fixed cell imaging suggests that the Cx36-Halo construct can successfully migrate to the plasma membrane and form gap junctions. We labeled the HaloTag protein with HaloTag TMR ligand, which formed irreversible covalent bonds with the HaloTag protein. Expression of Cx36-Halo construct is the most efficient 24 hours after transfection in HeLa cells. Double labeling of HaloTag ligand and Cx36 antibody confirmed that imaging with HaloTag ligand is efficient and sufficient to label Cx36 gap junction. To confirm that the insertion of HaloTag protein did not alter the properties of Cx36, we performed a scrape loading experiment to see how gap junctions formed by Cx36-Halo construct are regulated by PKA activity. Wild-type Cx36 gap junction coupling is inhibited by activation of PKA and vice versa. Our scrape loading experiment confirmed that Cx36-Halo gap junctions are regulated by PKA the same way as the wild-type Cx36 gap junction.

   Pulse-chase analysis is the most common way to study turn over rate of a protein in cell cultures. With the Cx36-Halo construct, we were able to label Cx36 at two different time point efficiently and specifically. Our results demonstrated that Cx36 migrates to and

away from the gap junction plaque with a half life of 2.8 hours, which is consistent with prior studies of turnover rates of other connexins.

Most connexins are synthesized in the ER, modified in the Golgi apparatus and TGN, and finally inserted into the plasma membrane, where they dock with hemichannels from the adjacent cell membrane. We repeated the pulse-chase analysis with treatment of BFA, which disrupted the TGN, and successfully prevented the addition of new connexins into the gap junction plague. This confirmed that Cx36 travels through the traditional ER-Golgi-TGN-plasma membrane in order to form gap junction plaque.

Previous studies have reported that connexons are incorporated in the gap junction as undocked hemichannels packaged in vesicles (Gaietta et al., 2002) (Lauf et al., 2002), and removed as paired channels that form a double membrane vesicle known as annular junction (Laird, 1996) (Gaietta et al., 2002) (Laird, 1996) (Lauf et al., 2002). These annular gap junctions subsequently are transported to lysosomes, where they are degraded (Laird, 1996) (Piehl et al., 2007). Our microscopic evidence is consistent with this theory by showing two different classes of vesicles: the small synthesis vesicles for exocytosis and the large ring shaped vesicles for endocytosis. Future studies could be done to verify the identities of two classes of vesicles. We could do electron microscopy to see whether the vesicles are single or double membrane vesicles. We could also double-label Cx36-Halo with lysosomal markers to identify the removal vesicles.

Factors influencing turnover rate studies

Although our reported half-life of Cx36 in HeLa cells is consistent with the studies of other connexins in cell cultures and whole organs (Herve et al., 2007), as well as the electrophysiology data of Cx36 half-life in Mauthner cells reported by the Pereda group (Flores et al., 2012), there are still considerable factors that may influence the measurement of half-lives. Turnover rate of plasma membrane proteins have been reported to be very different in different cell types. It is believed that the turnover rate of a certain protein can be cell type specific instead of protein specific. For example, Cx32 showed a half-life of 4-6 hours in rat hepatocytes (Traub and Wong, 1983), but only 2.5-3 hours in mouse embryo hepatocytes (Traub et al., 1987), suggesting that Cx32 gap junctions turn over faster in embryo cells. When turnover rate studies are carried out in primary cultures of cells, cells may contain intact gap junctions from their previous neighbors before cell division and isolation, and these gap junctions are removed and internalized in a very rapid rate (Herve et al., 2007). In these conditions, connexin turnover rate might be faster in cell cultures than intact tissues. However, pulse-chase analysis showed that Cx43 had similar half-life in metabolically labeled rat heart (Beardslee et al., 1998) and cultured myocytes (Laird et al., 1991) (Darrow et al., 1995) (Laing et al., 1998). In some cases, connexins in primary cell culture even showed a slower turnover rate, i.e. Cx45 reported a half-life of 4.2 hours in HeLa cells (Hertlein et al., 1998), but only 2.9 hours in rat cardiac myocytes (Darrow et al., 1995).

Contribution of turnover to electrical synaptic plasticity

Connexin proteins have relatively fast turnover rates, with short half-lives of a few hours. The reasons for this fast turnover rate have remained elusive. It is possible that connexin proteins, like many other integral membrane proteins, have to constantly respond to physiological changes. Their up- or down-regulation in response to certain physiological changes may be crucial in cell survival. One example is given by the hyperglycemia enhanced degradation of Cx43 in bovine retinal endothelial cells, where half-life of Cx43 reduced from 2.3 hours to 1.9 hours (Fernandes et al., 2004). This implied that natural stress, like oxidative or heat stress, can affect the turnover rate of connexins.

In previous studies, the numbers and size of Cx36 has been assessed in different conditions with different treatments. Kothmann et al. showed that phosphorylation of regulatory sites on Cx36 did not alter trafficking and distribution of the protein. Cx36 plaque size and number of Cx36 plaques per unit area remained the same after treatment of dopamine receptor agonist and antagonist on AII amacrine cell dendrites in IPL of rabbit retina while tracer coupling changed 20-fold (Kothmann et al., 2009). Li et al. also showed that the number of Cx36 plaques per unit area in the OPL was not affected by light or dark adaptation of the mouse retina while coupling changed dramatically (Li et al., 2013). One recent publication from the Sekaran lab showed that Cx36 protein level was regulated by diurnal and circadian rhythm (Katti et al., 2013). The level of Cx36 transcript peaked in the late night phase and immune-labeling showed a higher Cx36 expression level in the night phase than in the day in the OPL of mouse retina. This contradicts the findings in the Li et al. paper where number of Cx36 gap junction plaques did not change with time of day. Sekaran lab measured the amount of Cx36 present with western blot and Cx36 transcript

expression level, which could be measuring a combination of membrane and intracellular pool of proteins. It reflected the fluctuation in Cx36 protein syntheis rate, which could be contributing to the change in protein level.

The turnover rate we observed is too slow to contribute substantially to short-term changes in coupling of neurons driven by transmitters such as dopamine, which take minutes to achieve. But with further physiological and electrophysiological studies, we may be able to show that Cx36 turnover rate contributes to long-term plasticity in electrical synaptic strength. Katti et al. suggested that turnover of Cx36 was more likely affected in the protein synthesis and transcriptional level with diurnal and circadian regulation. It is possible that Cx36 turnover rate changes to alter long term plasticity in response to the change in levels neurotransmitters such as dopamine and adenosine, which are key regulators in Cx36 gap junction coupling (Li et al., 2009a) (Kothmann et al., 2009) (Li et al., 2013). With HaloTag technology, we can use the metabolic labeling and pulse-chase analysis to further study Cx36 turnover rate in different conditions and its role in electrical synapse plasticity.

Bibliography

Ahmad, S., Diez, J.A., George, C.H., and Evans, W.H. (1999a). Synthesis and assembly of connexins in vitro into homomeric and heteromeric functional gap junction hemichannels. The Biochemical journal *339*, 247-253.

Ahmad, S., Diez, J.A., George, C.H., and Evans, W.H. (1999b). Synthesis and assembly of connexins in vitro into homomeric and heteromeric functional gap junction hemichannels. The Biochemical journal *339 (Pt 2)*, 247-253.

Ahmad, S., and Evans, W.H. (2002). Post-translational integration and oligomerization of connexin 26 in plasma membranes and evidence of formation of membrane pores: implications for the assembly of gap junctions. The Biochemical journal *365*, 693-699.

Al-Ubaidi, M.R., White, T.W., Ripps, H., Poras, I., Avner, P., Gomes, D., and Bruzzone, R. (2000). Functional properties, developmental regulation, and chromosomal localization of murine connexin36, a gap-junctional protein expressed preferentially in retina and brain. Journal of neuroscience research *59*, 813-826.

Alev, C., Urschel, S., Sonntag, S., Zoidl, G., Fort, A.G., Hoher, T., Matsubara, M., Willecke, K., Spray, D.C., and Dermietzel, R. (2008). The neuronal connexin36 interacts with and is phosphorylated by CaMKII in a way similar to CaMKII interaction with glutamate receptors. Proceedings of the National Academy of Sciences of the United States of America *105*, 20964-20969.

Beardslee, M.A., Laing, J.G., Beyer, E.C., and Saffitz, J.E. (1998). Rapid turnover of connexin43 in the adult rat heart. Circ Res *83*, 629-635.

Belluardo, N., Mudo, G., Trovato-Salinaro, A., Le Gurun, S., Charollais, A., Serre-Beinier, V., Amato, G., Haefliger, J.A., Meda, P., and Condorelli, D.F. (2000). Expression of connexin36 in the adult and developing rat brain. Brain Res *865*, 121-138.

Berthoud, V.M., Bassnett, S., and Beyer, E.C. (1999). Cultured chicken embryo lens cells resemble differentiating fiber cells in vivo and contain two kinetic pools of connexin56. Exp Eye Res *68*, 475-484.

Blatow, M., Rozov, A., Katona, I., Hormuzdi, S.G., Meyer, A.H., Whittington, M.A., Caputi, A., and Monyer, H. (2003). A novel network of multipolar bursting interneurons generates theta frequency oscillations in neocortex. Neuron *38*, 805-817.

Bloomfield, S.A., and Volgyi, B. (2009). The diverse functional roles and regulation of neuronal gap junctions in the retina. Nat Rev Neurosci *10*, 495-506.

Breidert, S., Jacob, R., Ngezahayo, A., Kolb, H.A., and Naim, H.Y. (2005). Trafficking pathways of Cx49-GFP in living mammalian cells. Biological chemistry *386*, 155-160.

Christie, J.M., Bark, C., Hormuzdi, S.G., Helbig, I., Monyer, H., and Westbrook, G.L. (2005). Connexin36 mediates spike synchrony in olfactory bulb glomeruli. Neuron *46*, 761-772.

Condorelli, D.F., Belluardo, N., Trovato-Salinaro, A., and Mudo, G. (2000). Expression of Cx36 in mammalian neurons. Brain Res Brain Res Rev *32*, 72-85.

Darrow, B.J., Laing, J.G., Lampe, P.D., Saffitz, J.E., and Beyer, E.C. (1995). Expression of multiple connexins in cultured neonatal rat ventricular myocytes. Circulation Research *76*, 381-387.

De Zeeuw, C.I., Chorev, E., Devor, A., Manor, Y., Van Der Giessen, R.S., De Jeu, M.T., Hoogenraad, C.C., Bijman, J., Ruigrok, T.J., French, P.*, et al.* (2003). Deformation of network connectivity in the inferior olive of connexin 36-deficient mice is compensated by morphological and electrophysiological changes at the single neuron level. The Journal of neuroscience : the official journal of the Society for Neuroscience *23*, 4700-4711.

Deans, M.R., Gibson, J.R., Sellitto, C., Connors, B.W., and Paul, D.L. (2001). Synchronous activity of inhibitory networks in neocortex requires electrical synapses containing connexin36. Neuron *31*, 477-485.

Deans, M.R., Volgyi, B., Goodenough, D.A., Bloomfield, S.A., and Paul, D.L. (2002). Connexin36 is essential for transmission of rod-mediated visual signals in the mammalian retina. Neuron *36*, 703-712.

Diestel, S., Eckert, R., Hulser, D., and Traub, O. (2004). Exchange of serine residues 263 and 266 reduces the function of mouse gap junction protein connexin31 and exhibits a

dominant-negative effect on the wild-type protein in HeLa cells. Experimental cell research *294*, 446-457.

Evans, W.H., Ahmad, S., Diez, J., George, C.H., Kendall, J.M., and Martin, P.E. (1999). Trafficking pathways leading to the formation of gap junctions. Novartis Foundation symposium *219*, 44-54; discussion 54-49.

Falk, M.M., Buehler, L.K., Kumar, N.M., and Gilula, N.B. (1997). Cell-free synthesis and assembly of connexins into functional gap junction membrane channels. The EMBO journal *16*, 2703-2716.

Falk, M.M., and Gilula, N.B. (1998). Connexin membrane protein biosynthesis is influenced by polypeptide positioning within the translocon and signal peptidase access. The Journal of biological chemistry *273*, 7856-7864.

Falk, M.M., Kumar, N.M., and Gilula, N.B. (1994). Membrane insertion of gap junction connexins: polytopic channel forming membrane proteins. The Journal of cell biology *127*, 343-355.

Fallon, R.F., and Goodenough, D.A. (1981). Five-hour half-life of mouse liver gap-junction protein. The Journal of cell biology *90*, 521-526.

Fernandes, R., Girao, H., and Pereira, P. (2004). High glucose down-regulates intercellular communication in retinal endothelial cells by enhancing degradation of connexin 43 by a proteasome-dependent mechanism. The Journal of biological chemistry *279*, 27219-27224.

Fishman, G.I., Gao, Y., Hertzberg, E.L., and Spray, D.C. (1995). Reversible intercellular coupling by regulated expression of a gap junction channel gene. Cell adhesion and communication *3*, 353-365.

Flores, C.E., Nannapaneni, S., Davidson, K.G., Yasumura, T., Bennett, M.V., Rash, J.E., and Pereda, A.E. (2012). Trafficking of gap junction channels at a vertebrate electrical synapse in vivo. Proceedings of the National Academy of Sciences of the United States of America *109*, E573-582.

G. Los, R.L., Natasha Karassina, Chad Zimprich, Mark G. McDougall, Lance P. Encell, Rachel Friedman-Ohana, Monika Wood, Gediminas Vidugiris, Kris Zimmerman, Paul Otto, Soshana Berstock, Dieter Klaubert,and Ketih V. Wood (2006). HaloTag® Technology: Cell Imaging and Protein Analysis. Cell Notes *14*, 10-14.

Gaietta, G., Deerinck, T.J., Adams, S.R., Bouwer, J., Tour, O., Laird, D.W., Sosinsky, G.E., Tsien, R.Y., and Ellisman, M.H. (2002). Multicolor and electron microscopic imaging of connexin trafficking. Science *296*, 503-507.

George, C.H., Kendall, J.M., and Evans, W.H. (1999). Intracellular trafficking pathways in the assembly of connexins into gap junctions. The Journal of biological chemistry *274*, 8678-8685.

George, C.H., Martin, P.E., and Evans, W.H. (1998). Rapid determination of gap junction formation using HeLa cells microinjected with cDNAs encoding wild-type and chimeric connexins. Biochemical and biophysical research communications *247*, 785-789.

Georgyi V. Los, A.D., Natasha Karassina, Chad Zimprich, Randall Learish, Mark G. McDougall, Lance P. Encell, Rachel Friedman-Ohana, Monika Wood, Gediminas Vidugiris, Kris Zimmerman, Paul Otto, Dieter H. Klaubert, and Keith V. Wood (2005). HaloTag® Interchangeable Labeling Technology for Cell Imaging and Protein Capture. Cell Notes *11*, 2-6.

He, L.Q., Cai, F., Liu, Y., Liu, M.J., Tan, Z.P., Pan, Q., Fang, F.Y., Liang de, S., Wu, L.Q., Long, Z.G.*, et al.* (2005). Cx31 is assembled and trafficked to cell surface by ER-Golgi pathway and degraded by proteasomal or lysosomal pathways. Cell research *15*, 455-464.

Hertlein, B., Butterweck, A., Haubrich, S., Willecke, K., and Traub, O. (1998). Phosphorylated carboxy terminal serine residues stabilize the mouse gap junction protein connexin45 against degradation. The Journal of membrane biology *162*, 247-257.

Hertzberg, E.L., Saez, J.C., Corpina, R.A., Roy, C., and Kessler, J.A. (2000). Use of antibodies in the analysis of connexin 43 turnover and phosphorylation. Methods *20*, 129-139.

Herve, J.C., Derangeon, M., Bahbouhi, B., Mesnil, M., and Sarrouilhe, D. (2007). The connexin turnover, an important modulating factor of the level of cell-to-cell junctional communication: comparison with other integral membrane proteins. The Journal of membrane biology *217*, 21-33.

Hormuzdi, S.G., Pais, I., LeBeau, F.E., Towers, S.K., Rozov, A., Buhl, E.H., Whittington, M.A., and Monyer, H. (2001). Impaired electrical signaling disrupts gamma frequency oscillations in connexin 36-deficient mice. Neuron *31*, 487-495.

Hunter, A.W., Barker, R.J., Zhu, C., and Gourdie, R.G. (2005). Zonula occludens-1 alters connexin43 gap junction size and organization by influencing channel accretion. Molecular biology of the cell *16*, 5686-5698.

Katti, C., Butler, R., and Sekaran, S. (2013). Diurnal and circadian regulation of connexin 36 transcript and protein in the Mammalian retina. Investigative ophthalmology & visual science *54*, 821-829.

Kothmann, W.W., Li, X., Burr, G.S., and O'Brien, J. (2007). Connexin 35/36 is phosphorylated at regulatory sites in the retina. Visual neuroscience *24*, 363-375.

Kothmann, W.W., Massey, S.C., and O'Brien, J. (2009). Dopamine-stimulated dephosphorylation of connexin 36 mediates AII amacrine cell uncoupling. The Journal of neuroscience : the official journal of the Society for Neuroscience *29*, 14903-14911.

Koval, M., Harley, J.E., Hick, E., and Steinberg, T.H. (1997). Connexin46 is retained as monomers in a trans-Golgi compartment of osteoblastic cells. The Journal of cell biology *137*, 847-857.

Kumar, N.M., and Gilula, N.B. (1992). Molecular biology and genetics of gap junction channels. Seminars in cell biology *3*, 3-16.

Laing, J.G., and Beyer, E.C. (1995). The gap junction protein connexin43 is degraded via the ubiquitin proteasome pathway. The Journal of biological chemistry *270,* 26399-26403.

Laing, J.G., Tadros, P.N., Green, K., Saffitz, J.E., and Beyer, E.C. (1998). Proteolysis of connexin43-containing gap junctions in normal and heat-stressed cardiac myocytes. Cardiovasc Res *38,* 711-718.

Laing, J.G., Tadros, P.N., Westphale, E.M., and Beyer, E.C. (1997). Degradation of connexin43 gap junctions involves both the proteasome and the lysosome. Experimental cell research *236,* 482-492.

Laird, D.W. (1996). The life cycle of a connexin: gap junction formation, removal, and degradation. J Bioenerg Biomembr *28,* 311-318.

Laird, D.W., Castillo, M., and Kasprzak, L. (1995). Gap junction turnover, intracellular trafficking, and phosphorylation of connexin43 in brefeldin A-treated rat mammary tumor cells. The Journal of cell biology *131*, 1193-1203.

Laird, D.W., Puranam, K.L., and Revel, J.P. (1991). Turnover and phosphorylation dynamics of connexin43 gap junction protein in cultured cardiac myocytes. The Biochemical journal *273(Pt 1)*, 67-72.

Lampe, P.D. (1994). Analyzing phorbol ester effects on gap junctional communication: a dramatic inhibition of assembly. The Journal of cell biology *127*, 1895-1905.

Larson, D.M., Seul, K.H., Berthoud, V.M., Lau, A.F., Sagar, G.D., and Beyer, E.C. (2000). Functional expression and biochemical characterization of an epitope-tagged connexin37. Mol Cell Biol Res Commun *3*, 115-121.

Larson, D.M., Wrobleski, M.J., Sagar, G.D., Westphale, E.M., and Beyer, E.C. (1997). Differential regulation of connexin43 and connexin37 in endothelial cells by cell density, growth, and TGF-beta1. Am J Physiol *272*, C405-415.

Lauf, U., Giepmans, B.N., Lopez, P., Braconnot, S., Chen, S.C., and Falk, M.M. (2002). Dynamic trafficking and delivery of connexons to the plasma membrane and accretion to gap junctions in living cells. Proceedings of the National Academy of Sciences of the United States of America *99*, 10446-10451.

Li, H., Chuang, A.Z., and O'Brien, J. (2009a). Photoreceptor coupling is controlled by connexin 35 phosphorylation in zebrafish retina. The Journal of neuroscience : the official journal of the Society for Neuroscience *29*, 15178-15186.

Li, H., Zhang, Z., Blackburn, M.R., Wang, S.W., Ribelayga, C.P., and O'Brien, J. (2013). Adenosine and dopamine receptors coregulate photoreceptor coupling via gap junction phosphorylation in mouse retina. The Journal of neuroscience : the official journal of the Society for Neuroscience *33*, 3135-3150.

Li, X., Lu, S., and Nagy, J.I. (2009b). Direct association of connexin36 with zonula occludens-2 and zonula occludens-3. Neurochem Int *54*, 393-402.

Li, X., Lynn, B.D., and Nagy, J.I. (2012). The effector and scaffolding proteins AF6 and MUPP1 interact with connexin36 and localize at gap junctions that form electrical synapses in rodent brain. The European journal of neuroscience *35*, 166-181.

Li, X., Olson, C., Lu, S., Kamasawa, N., Yasumura, T., Rash, J.E., and Nagy, J.I. (2004). Neuronal connexin36 association with zonula occludens-1 protein (ZO-1) in mouse brain and interaction with the first PDZ domain of ZO-1. The European journal of neuroscience *19*, 2132-2146.

Long, M.A., Deans, M.R., Paul, D.L., and Connors, B.W. (2002). Rhythmicity without synchrony in the electrically uncoupled inferior olive. The Journal of neuroscience : the official journal of the Society for Neuroscience *22*, 10898-10905.

Los, G.V., Encell, L.P., McDougall, M.G., Hartzell, D.D., Karassina, N., Zimprich, C., Wood, M.G., Learish, R., Ohana, R.F., Urh, M.*, et al.* (2008). HaloTag: a novel protein labeling technology for cell imaging and protein analysis. ACS chemical biology *3*, 373-382.

Los, G.V., and Wood, K. (2007). The HaloTag: a novel technology for cell imaging and protein analysis. Methods in molecular biology *356*, 195-208.

Marandykina, A., Palacios-Prado, N., Rimkute, L., Skeberdis, V.A., and Bukauskas, F.F. (2013). Regulation of Connexin-36 Gap Junction Channels by n-Alkanols and Arachidonic Acid. The Journal of physiology.

Martin, P.E., Errington, R.J., and Evans, W.H. (2001). Gap junction assembly: multiple connexin fluorophores identify complex trafficking pathways. Cell communication & adhesion *8*, 243-248.

Mills, S.L., and Massey, S.C. (1998). The kinetics of tracer movement through homologous gap junctions in the rabbit retina. Visual neuroscience *15*, 765-777.

Musil, L.S., Cunningham, B.A., Edelman, G.M., and Goodenough, D.A. (1990). Differential phosphorylation of the gap junction protein connexin43 in junctional communication-competent and -deficient cell lines. The Journal of cell biology *111*, 2077-2088.

Musil, L.S., and Goodenough, D.A. (1993). Multisubunit assembly of an integral plasma membrane channel protein, gap junction connexin43, occurs after exit from the ER. Cell *74*, 1065-1077.

Musil, L.S., Le, A.C., VanSlyke, J.K., and Roberts, L.M. (2000). Regulation of connexin degradation as a mechanism to increase gap junction assembly and function. The Journal of biological chemistry *275*, 25207-25215.

O'Brien, J., Nguyen, H.B., and Mills, S.L. (2004). Cone photoreceptors in bass retina use two connexins to mediate electrical coupling. The Journal of neuroscience : the official journal of the Society for Neuroscience *24*, 5632-5642.

Ouyang, X., Winbow, V.M., Patel, L.S., Burr, G.S., Mitchell, C.K., and O'Brien, J. (2005). Protein kinase A mediates regulation of gap junctions containing connexin35 through a complex pathway. Brain Res Mol Brain Res *135*, 1-11.

Piehl, M., Lehmann, C., Gumpert, A., Denizot, J.P., Segretain, D., and Falk, M.M. (2007). Internalization of large double-membrane intercellular vesicles by a clathrin-dependent endocytic process. Molecular biology of the cell *18*, 337-347.

Saez, J.C., Berthoud, V.M., Branes, M.C., Martinez, A.D., and Beyer, E.C. (2003). Plasma membrane channels formed by connexins: their regulation and functions. Physiological reviews *83*, 1359-1400.

Srinivas, M., Rozental, R., Kojima, T., Dermietzel, R., Mehler, M., Condorelli, D.F., Kessler, J.A., and Spray, D.C. (1999). Functional properties of channels formed by the neuronal gap junction protein connexin36. The Journal of neuroscience : the official journal of the Society for Neuroscience *19*, 9848-9855.

Thomas, M.A., Huang, S., Cokoja, A., Riccio, O., Staub, O., Suter, S., and Chanson, M. (2002). Interaction of connexins with protein partners in the control of channel turnover and gating. Biology of the cell / under the auspices of the European Cell Biology Organization *94*, 445-456.

Thomas, T., Jordan, K., Simek, J., Shao, Q., Jedeszko, C., Walton, P., and Laird, D.W. (2005). Mechanisms of Cx43 and Cx26 transport to the plasma membrane and gap junction regeneration. Journal of cell science *118*, 4451-4462.

Traub, O., Look, J., Dermietzel, R., Brummer, F., Hulser, D., and Willecke, K. (1989). Comparative characterization of the 21-kD and 26-kD gap junction proteins in murine liver and cultured hepatocytes. The Journal of cell biology *108*, 1039-1051.

Traub, O., Look, J., Paul, D., and Willecke, K. (1987). Cyclic adenosine monophosphate stimulates biosynthesis and phosphorylation of the 26 kDa gap junction protein in cultured mouse hepatocytes. Eur J Cell Biol *43*, 48-54.

Traub, R.D., and Wong, R.K. (1983). Synaptic mechanisms underlying interictal spike initiation in a hippocampal network. Neurology *33*, 257-266.

VanSlyke, J.K., Deschenes, S.M., and Musil, L.S. (2000). Intracellular transport, assembly, and degradation of wild-type and disease-linked mutant gap junction proteins. Molecular biology of the cell *11*, 1933-1946.

Willecke, K., Eiberger, J., Degen, J., Eckardt, D., Romualdi, A., Guldenagel, M., Deutsch, U., and Sohl, G. (2002). Structural and functional diversity of connexin genes in the mouse and human genome. Biological chemistry *383*, 725-737.

Windoffer, R., Beile, B., Leibold, A., Thomas, S., Wilhelm, U., and Leube, R.E. (2000). Visualization of gap junction mobility in living cells. Cell Tissue Res *299*, 347-362.

Yamaguchi, D.T., and Ma, D. (2003). Mechanism of pH regulation of connexin 43 expression in MC3T3-E1 cells. Biochemical and biophysical research communications *304*, 736-739.

Yin, X., Jedrzejewski, P.T., and Jiang, J.X. (2000). Casein kinase II phosphorylates lens connexin 45.6 and is involved in its degradation. The Journal of biological chemistry *275*, 6850-6856.

Zhang, J.T., Chen, M., Foote, C.I., and Nicholson, B.J. (1996). Membrane integration of in vitro-translated gap junctional proteins: co- and post-translational mechanisms. Molecular biology of the cell *7*, 471-482.

Zimmerman, A.L., and Rose, B. (1985). Permeability properties of cell-to-cell channels: kinetics of fluorescent tracer diffusion through a cell junction. The Journal of membrane biology *84*, 269-283.

VITA

Yanran Wang (Helen) was born in Nanjing, China on October 13th, 1984, the daughter of Xudong Wang, MD and Xianhong Zhou. After completing her work at Dunman High School and Raffles Junior College in Singapore, she entered St. Mary's University in San Antonio, Texas in January 2004. She received the degree of Bachelor of Science, majoring in chemistry and Biology, in 2007. She worked as a research assistant at Texas Biomedical Research Institute (previously known as Southwest Foundation for Biomedical Research) from 2006 to 2007. In May of 2009 she entered the neuroscience program at The University of Texas Health Science Center at Houston Graduate School of Biomedical Sciences.

Permanent address:

1601 Castle Ct, Apt 6

Houston, Texas 77006